Title: Pharmacological manipulations of physiological arousal and sleep-like slow waves modulate sustained attention

Authors: Elaine Pinggal[1], Paul M. Dockree[2], Redmond G. O'Connell[2], Mark A. Bellgrove[1]* & Thomas Andrillon[3,4]*

*: equal contribution

Affiliations:

1. School of Psychological Sciences, Turner Institute for Brain and Mental Health, Monash University, Melbourne 3168, Victoria, Australia.
2. Trinity College Institute of Neuroscience & School of Psychology, Trinity College Dublin, Dublin, Ireland.
3. School of School of Philosophical, Historical, and International Studies, Centre for Consciousness and Contemplative Studies, Monash University, Melbourne 3168, Victoria, Australia.
4. Paris Brain Institute, Sorbonne Université, Inserm-CNRS, Paris, 75013, France.

Corresponding author: Thomas Andrillon.
Postal Address: Paris Brain Institute, Hôpital Pitié-Salpêtrière, 47 Bd de l'Hôpital, 75013 Paris, France.
Email: thomas.andrillon@icm-institute.org
ORCID: https://orcid.org/0000-0003-2794-8494

Abstract

Sustained attention describes our ability to keep a constant focus on a given task. This ability is modulated by our physiological state of arousal. Although lapses of sustained attention have been linked with dysregulations of arousal, the underlying physiological mechanisms remain unclear. An emerging body of work proposes that the intrusion during wakefulness of sleep-like slow waves, a marker of the transition toward sleep, could mechanistically account for attentional lapses. This study aimed to expose, via pharmacological manipulations of the monoamine system, the relationship between the occurrence of sleep-like slow waves and the behavioural consequences of sustained attention failures. In a double-blind, randomised-control trial, 32 healthy participants received methylphenidate, atomoxetine, citalopram or placebo during four separate experimental sessions. During each session, electroencephalography (EEG) was used to measure neural activity whilst participants completed a visual task requiring sustained attention. Methylphenidate, which increases wake-promoting dopamine and noradrenaline across cortical and subcortical areas, improved behavioural performance whereas atomoxetine, which increases dopamine and noradrenaline predominantly over frontal cortices, led to more impulsive responses. Additionally, citalopram, which increases sleep-promoting serotonin, led to more missed trials. Based on EEG recording, citalopram was also associated with an increase in sleep-like slow waves. Importantly, compared to a classical marker of arousal such as alpha power, only slow waves differentially predicted both slower and faster responses in a region-specific fashion. These results suggest that a decrease in arousal can lead to local sleep intrusions during wakefulness which could be mechanistically linked to impulsivity and sluggishness.

Introduction

Sustained attention refers to the ability to concentrate cognitive resources on a given task or specific stimuli for extended periods of time (van Schie et al., 2021). Previous research has emphasised the capacity limits of this ability, especially when the task at hand is easy and repetitive or when individuals are unmotivated (Esterman and Rothlein, 2019). This difficulty in maintaining a continuous attentional focus goes beyond lab studies, with an estimated 50% of our waking time spent not focusing on the task at hand (Killingsworth and Gilbert, 2010). Fluctuations of attention impact performance in a complex fashion, leading to a mixture of unresponsiveness, sluggishness and impulsivity (O'Connell et al., 2009; Oken et al., 2006; Riley et al., 2017). Fluctuating attention also impacts subjective experience, resulting in phenomena such as mind wandering (i.e. thinking about something else than the task at hand) (Smallwood and Schooler, 2015) or mind blanking (i.e. thinking about nothing at all) (Ward and Wegner, 2013).

Failures to maintain sustained attention vary with fluctuations in physiological arousal, defined here as the physiological state that allows encoding, processing, and responding to environmental stimuli. Indeed, on the one hand, attentional failures have been associated with hypo-arousal as they increase with fatigue and time spent awake (Riley et al., 2017) and are very sensitive to sleep deprivation (Doran et al., 2001). On the other hand, an excess of arousal (hyper-arousal) also appears detrimental to sustained attention (Mittner et al., 2016). For example, mind wandering has been associated with increased baseline pupil dilation (a marker of physiological arousal) compared to task-focused states (Smallwood et al., 2011). In addition, hypo- and hyper-arousal have been hypothesised to be linked as states of hyper-arousal could serve to transiently offset a baseline state of hypo-arousal. For example, individuals with attentional deficits (e.g. Attention Deficit Hyperactivity Disorder, ADHD) may experience low levels of arousal at rest (Satterfield and Dawson, 1971) and attentional deficits could stem from

76 a combination of a low-arousal baseline (e.g. low tonic dopaminergic activity) combined with
77 an autoregulatory attempt at compensating for this low baseline (e.g. high phasic dopaminergic
78 activity) (Geissler et al., 2014). At the level of cortical networks, intermediate levels of arousal
79 could promote optimal levels of sustained attention by balancing levels of excitation and
80 inhibition (Oken et al., 2006). Interestingly, the neuromodulators involved in the regulation of
81 physiological arousal and sleep-wake transitions (Jones, 2005; Oken et al., 2006; Thiele and
82 Bellgrove, 2018) are also involved in the regulation of sustained attention (Oken et al., 2006;
83 Thiele and Bellgrove, 2018).

84 Arousal is regulated by a number of neuromodulators, which include (but is not limited
85 to) noradrenaline, dopamine and serotonin (Thiele and Bellgrove, 2018). These
86 neuromodulators have well-documented effects on attention by, for example, optimising neural
87 responses to the environment (Ranjbar-Slamloo and Fazlali, 2020) or promoting prefrontal
88 cortical processing (Robbins, 1997; Thiele and Bellgrove, 2018).

89 First, noradrenaline is one of the key neuromodulators allowing global transitions from
90 wakefulness to sleep and vice versa (Jones, 2005). Noradrenaline release leads to broad cortical
91 activation via the inhibition of sleep-promoting systems and the activation of wake-promoting
92 systems. The widespread cortical release of noradrenaline by the Locus Coeruleus (LC) is
93 maximal during wakefulness, decreases in Non-Rapid Eye Movement (NREM) sleep and
94 vanishes in Rapid Eye Movement (REM) sleep. Additionally, noradrenaline is released
95 following the occurrence of novel or salient stimuli and can decrease response thresholds and
96 improve the efficiency of synaptic transmissions by modifying the cellular properties of target
97 neurons (Robbins, 1997; Ross and Van Bockstaele, 2021; Sara, 2009). A previous report on
98 the same dataset as we present here, showed that an increase of noradrenaline and dopamine
99 via methylphenidate led to enhanced responses to visual stimuli and a reduction of alpha
100 oscillations (Dockree et al., 2017). However, too much noradrenergic activity (as for example

101 during high stress situations) can also lead to an impairment of executive functions and
102 behaviour (Arnsten, 2010, 2000). Finally, another recent study found that decreasing the
103 concentration of noradrenaline through pharmacological challenge led to an increase in
104 drowsiness, decreased performance in a visual task and weaker sensory responses whereas
105 increasing noradrenaline had the opposite effect (Gelbard-Sagiv et al., 2018), confirming that
106 the impact of noradrenaline on performance is U-shaped (Sara and Bouret, 2012).

107 Second, the relationship between dopamine and cognitive performance also follows an
108 inverted U-shape, with the best cognitive performance being observed when dopamine levels
109 are at an intermediate level (Maffei and Angrilli, 2018). However, the impact of dopamine on
110 arousal is difficult to separate from that of noradrenaline (Lee and Dan, 2012; Robbins, 1997).
111 Both noradrenaline and dopamine innervate related areas, share biosynthetic and intracellular
112 signalling pathways, and are occasionally released simultaneously from noradrenergic
113 terminals such as the LC (Ranjbar-Slamloo and Fazlali, 2020). An integrative model of the role
114 of noradrenaline and dopamine posits that dopamine decreases the amount of noise whereas
115 noradrenaline enhances signal, participating thus in a complementary process to increase the
116 signal-to-noise ratio (Arnsten and Rubia, 2012). Importantly, like noradrenaline, dopamine
117 also influences physiological arousal and promotes wakefulness (Boutrel and Koob, 2004). In
118 fact, early treatments against narcolepsy included stimulant drugs such as methylphenidate,
119 which increase the levels of dopamine and noradrenaline (Mignot, 2012) and is also used in
120 the treatment of attentional disorders (Arnsten, 2010; Cortese, 2020).

121 Third, some evidence also suggests that serotonin may play a role in the regulation of
122 arousal. For instance, serotonin may influence the regulation of sleep and wakefulness as the
123 raphe nuclei releases serotonin maximally during wakefulness, less during NREM sleep and
124 ceases firing during REM sleep (Jones, 2005). These effects have been interpreted as serotonin
125 stimulating wakefulness (Jones, 2005), however, a recent study by Oikonomou et al. (2019)

suggests a role for serotonin in facilitating sleep onset. Accordingly, serotonin could be involved in the homeostatic regulation of sleep and its high concentration during wakefulness could be related to the build-up of sleep pressure during the day (Borbély et al., 2016; Jouvet, 1999). Serotonin also modulates attention directly or indirectly, by inhibiting, for example, the cholinergic system which plays a key role in the maintenance of attention (Jones, 2005; Sparks et al., 2018). Direct effects appear region or dose-specific (Thiele and Bellgrove, 2018) and low tonic activity in serotonin could improve attention by reducing impulsivity while high tonic activity could decrease the activation of prefrontal areas commonly activated in a sustained attention task (Sturm and Willmes, 2001; Wingen et al., 2008) and increase distractibility.

Although the neuromodulators mentioned above play a role in both the regulation of arousal and attention, these phenomena are often conceptualised and investigated separately. Here, we sought to explore whether the regulation of sleep/wake dynamics could be directly related to the modulation of sustained attention. For example, an increase in noradrenaline and/or dopamine could result in increased levels of physiological arousal, leading to cortical activation, improved signal-to-noise ratio of sensory responses, better intracortical communication, and lower response thresholds (Thiele and Bellgrove, 2018). Conversely, a decrease in arousal mediated by the same neuromodulators could negatively impact attention through the promotion of cortical idling (Pfurtscheller, 1992) or even sleep-like activity and cortical deactivation (Andrillon et al., 2019).

Electrophysiological (EEG) markers such as alpha oscillations have been used to investigate the relationship between physiological arousal and attention (Cajochen et al., 1995; Oken et al., 2006; Peylo et al., 2021). These oscillations are generated over the visual cortex and consist of sustained oscillatory activity with a frequency between 7 and 13 Hz (Clayton et al., 2018). A suppression of alpha oscillations has often been used as a proxy to estimate cortical excitability (Romei et al., 2008), a key component of physiological arousal, although

151 the generalisation of this relationship outside visual areas has been questioned (Samaha et al.,
152 2017). A study by O'Connell et al. (2009) found that alpha oscillations were a strong predictor
153 of attentional lapses, with an increase in alpha activity predicting lapses up to 20 seconds before
154 their occurrence. Alpha oscillations exemplify how modulations of arousal could impact
155 attention as increased levels of alpha oscillations could favour lapses of attention (Dockree et
156 al., 2017; O'Connell et al., 2009) by increasing cortical deactivation (Pfurtscheller et al., 1996).
157 Conversely, a decrease in alpha oscillations could favour enhanced cortical activation and
158 promote information processing (Klimesch et al., 2011; Peylo et al., 2021). However, the
159 relationship between alpha oscillations and arousal is not monotonic as alpha oscillations
160 decrease when individuals become drowsy or fall asleep (Kalauzi et al., 2012). In addition, the
161 associations between alpha oscillations and attention are task-dependent as increases in alpha
162 power have also been associated with the suppression of task-irrelevant distractors (Klimesch,
163 2012; Klimesch et al., 2011) and improved auditory processing (Dimitrijevic et al., 2017).
164 Thus, while the level of alpha oscillations have been robustly linked to sustained attention, this
165 relationship appears to be dependent on the nature of the task, the brain region over which it is
166 measured (Jensen and Mazaheri, 2010), and the baseline arousal state. Similarly, the
167 relationship between alpha oscillations and mind wandering appears complex, with an
168 influential study reporting less alpha during mind wandering (Braboszcz and Delorme, 2011)
169 whereas others found the reverse pattern (Arnau et al., 2020; Compton et al., 2019; Macdonald
170 et al., 2011).

171 To overcome these limitations, we examined the relationship between physiological
172 arousal and attention using a novel electroencephalographic (EEG) marker of arousal: sleep-
173 like slow waves occurring within wakefulness (Andrillon et al., 2019). Indeed, while sleep and
174 wakefulness are usually presented as mutually exclusive states, recent discoveries have shown
175 that sleep and wake activity can be concomitantly observed in different brain regions (Nir et

al., 2017; Nobili et al., 2012; Vyazovskiy et al., 2011). In particular, when one becomes fatigued, high amplitude slow oscillations (<7Hz), analogous to delta or theta sleep slow waves but smaller in amplitude, can be detected through EEG recordings (Andrillon et al., 2021; Bernardi et al., 2015; Hung et al., 2013). At the neuronal level, these waves are paired with momentary and localised periods of neuronal silencing (Vyazovskiy et al., 2011). These occurrences have been interpreted as "local sleep episodes" (Vyazovskiy et al., 2011), and could perturb information processing (Andrillon et al., 2019), following similar mechanisms that limit sensory processing and responsiveness during sleep (Andrillon and Kouider, 2020). Accordingly, these local sleep episodes have been shown to negatively impact behaviour (Bernardi et al., 2015; Hung et al., 2013; Vyazovskiy et al., 2011), notably in the context of tasks requiring sustained attention, and increase the frequency of mind wandering and mind blanking events (Andrillon et al., 2021). Importantly, these sleep-like slow waves are not restricted to contexts of acute sleep deprivation (Bernardi et al., 2015; Hung et al., 2013) but can also be found in well-rested individuals (Andrillon et al., 2021; Quercia et al., 2018). We aimed here to test if these slow waves varied as a function of pharmacological manipulation of key monoamine neuromodulators in well-rested individuals and could explain the relationship between fluctuations of arousal and attention.

To expose the relationship between the physiological substrates of sustained attention and arousal, monoamine (dopamine, noradrenaline and serotonin) agonists were administered to healthy, non-sedated participants while they performed a sustained attention EEG task (Figure 1). We re-analysed a dataset of participants who completed the Continuous Temporal Expectancy Task (CTET) (Dockree et al., 2017), a monotonous task wherein participants are required to monitor visual checkerboard stimuli for intermittent targets defined by their longer presentation (O'Connell et al., 2009). Methylphenidate (MPH) was used to increase both noradrenaline and dopamine levels globally across the cortex whilst atomoxetine (ATM) was

used to increase noradrenaline and dopamine more specifically in the prefrontal cortex (Bymaster, 2002; Chamberlain et al., 2009; Farr et al., 2014; Koda et al., 2010; Kowalczyk et al., 2019). Lastly, citalopram (CIT) was administered to increase serotonin. Only the results obtained with MPH have been previously reported, showing an improvement in sustained attention, a decrease in alpha oscillations and an increase in target detection (indexed via the P3 event-related potential), compared to placebo (Dockree et al., 2017). We expanded these findings by examining the impact of both arousal-promoting (MPH, ATM) and arousal-reducing (CIT) drugs. We also examined a more exhaustive set of EEG markers of attention and arousal, including physiological markers of sleep intrusions such as slow waves. We hypothesised that increasing noradrenaline and dopamine would lead to an increase in attention (decrease in attentional lapses) and arousal (less slow waves and alpha oscillations), whereas increasing serotonin would lead to impaired attention (increase in attentional lapses) and a decrease in arousal (more slow waves and alpha oscillations). Additionally, we hypothesised that slow waves and alpha oscillations would have differing roles in terms of their relationship with attentional lapses. Specifically, we hypothesised that in contrast to alpha oscillations which are generated within the occipital cortex, the behavioural impact of slow waves would vary as a function of their spatial location, with frontal slow waves being associated with impulsive behaviour (faster reaction times, more false alarms) and posterior slow waves being associated with sluggishness (slower reaction times, more misses) (Andrillon et al., 2021). Such a pattern of results would reinforce the idea that slow waves represent a neurophysiological mechanism underlying attentional lapses, in contrast to alpha oscillations which could more simply index an individual's level of arousal.

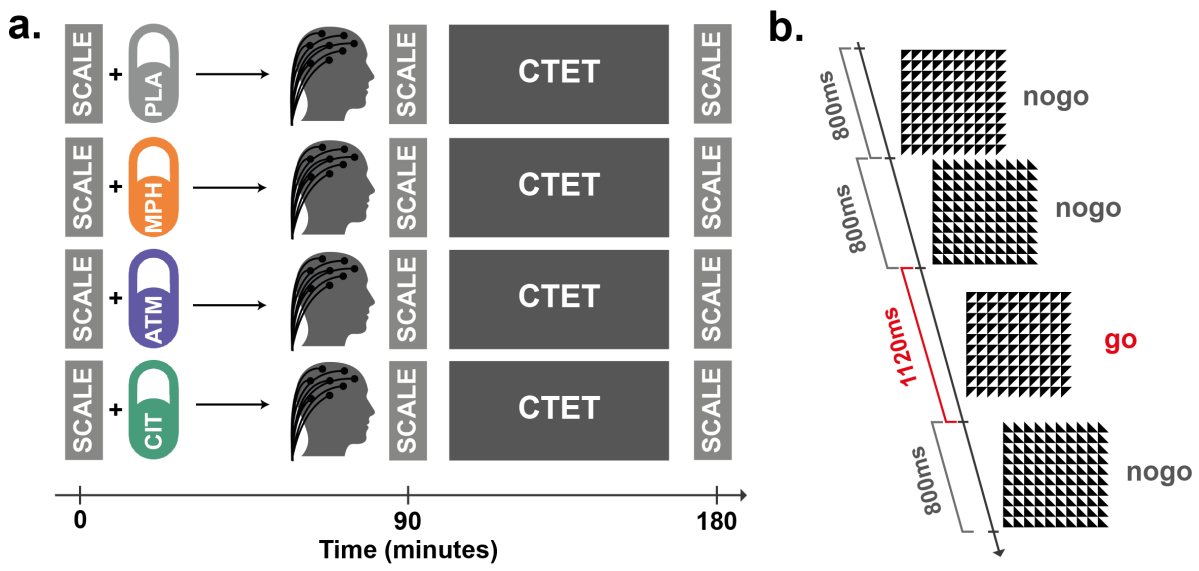

Figure 1. Experimental protocol.
a. *Each experimental session started with participants being administered one out of four treatments (PLA: placebo; MPH: methylphenidate; ATM: atomoxetine; CIT: citalopram) and completing the first Visual Analogue Scale (VAS) (time=0). The administration of the treatments was randomised across sessions (within-subject design). A second VAS was completed before starting the Continuous Temporal Expectancy Task (CTET), 90 minutes after treatment administration. Finally, after the CTET (and another task not analysed here) and 180 minutes after treatment administration, participants completed a third VAS. High-density EEG was recorded during the CTET.* ***b.*** *The CTET task was used to test sustained attention. In the CTET, participants are instructed to monitor a stream of visual stimuli (black and white checkboards) displayed on a screen placed in front of them. There are two types of stimuli: target stimuli for which participants are instructed to press a response button, and non-target stimuli that do not require a response. The only distinguishing factor between the non-target and target stimuli is the duration of the stimulus presentation (non-target: 800ms; target: 1120ms).*

Results

Subjective Sleepiness

To verify that the pharmacological interventions impacted subjective sleepiness, participants completed a visual analogue scale (VAS) three times during each experimental session: at drug administration (t=0 minutes), before the start of the sustained attention task (t=90 minutes), and after the task (t=180 minutes). A two-way repeated measures ANOVA was conducted to examine the effects of treatment (PLA, MPH, ATM, or CIT) and time (0, 90 and 180 minutes after drug administration; Figure S1) on subjective sleepiness. Thirty participants were included in this analysis after two subjects were excluded due to missing data (one experimental session missing in each participant, see Methods). This ANOVA revealed a main effect of time ($F(1.49, 43.28) = 22.4$, $p < .001$) and treatment ($F(3, 87) = 6.3$, $p < .001$) on sleepiness as well as a significant two-way interaction between treatment and time ($F(6, 174) = 6.5$, $p < .001$). Pairwise post-hoc comparisons by time points (t-tests, Bonferroni-corrected) indicated that there were no significant differences in sleepiness across drug treatment at the beginning of the protocol (drug administration: $F(3, 87) = 0.36$, $p_{adjusted} = 1$) but there were significant differences before and after the task ($F(3, 87) = 5.0$, $p_{adjusted} = .009$ and $F(3, 87) = 10.6$, $p_{adjusted} < .001$ resp.), confirming the effectiveness of the sustained attention protocol in engendering sleepiness. Pairwise post-hoc comparisons within treatments (t-tests, Bonferroni-corrected) indicated that this effect of treatment was driven by an absence of an increase in sleepiness for MPH, in keeping with the stimulant effect of MPH ($F(2, 58) = 2.0$, $p_{adjusted} = .59$), compared with PLA, CIT and ATM (all $p_{adjusted} < .01$). However, the administration of ATM or CIT did not significantly alter the subjective experience of sleepiness across the protocol compared with PLA.

264 **Sustained Attention Performance**

265 We next sought to examine the influence of the pharmacological manipulations on
266 behavioural measures of sustained attention. To do so, we examined behavioural performance
267 during the Continuous Temporal Expectancy Task (CTET), a task designed to monitor
268 participants' ability to pay careful attention to a continuous stream of visual information
269 (O'Connell et al., 2009). We focused on three behavioural variables: the proportion of missed
270 target trials (misses), the proportion of incorrect responses to non-target trials (false alarms)
271 and the reaction times for target trials (Figure 2).

272 To examine the performance across the entire CTET task (10 blocks), we fitted linear
273 mixed effect models to predict each of these variables of interest, with treatment as a
274 categorical fixed effect and subject identity as a categorical random effect (see Methods). We
275 compared these models with a null model, including only subject identity as a random effect
276 using the Likelihood Ratio Test, to test the effect of treatment on these behavioural variables.
277 These model comparisons revealed a strong effect of treatment on misses ($\chi^2(3) = 207.2$, $p <$
278 $.001$), false alarms ($\chi^2(3) = 52.1$, $p < .001$), and reaction times ($\chi^2(3) = 82.0$, $p < .001$).

279 Focusing on the winning models revealed that MPH, compared to PLA, was associated
280 with an improvement in behavioural performance across all three variables: less misses ($t = -$
281 10.5, $p < .001$), less false alarms ($t = -3.5$, $p < .001$) and faster reaction times ($t = -7.2$, $p < .001$).
282 This means that, under MPH, participants were faster and better at detecting target trials
283 without becoming too impulsive and responding to non-target trials. We applied the signal
284 detection theory (Macmillan, 1993) to combine responses on target and non-target trials in one
285 single index of behavioural performance (d'; Figure S2). MPH led to an increase in d' compared
286 to PLA ($t = 8.8$, $p < .001$), indicating enhanced sensitivity.

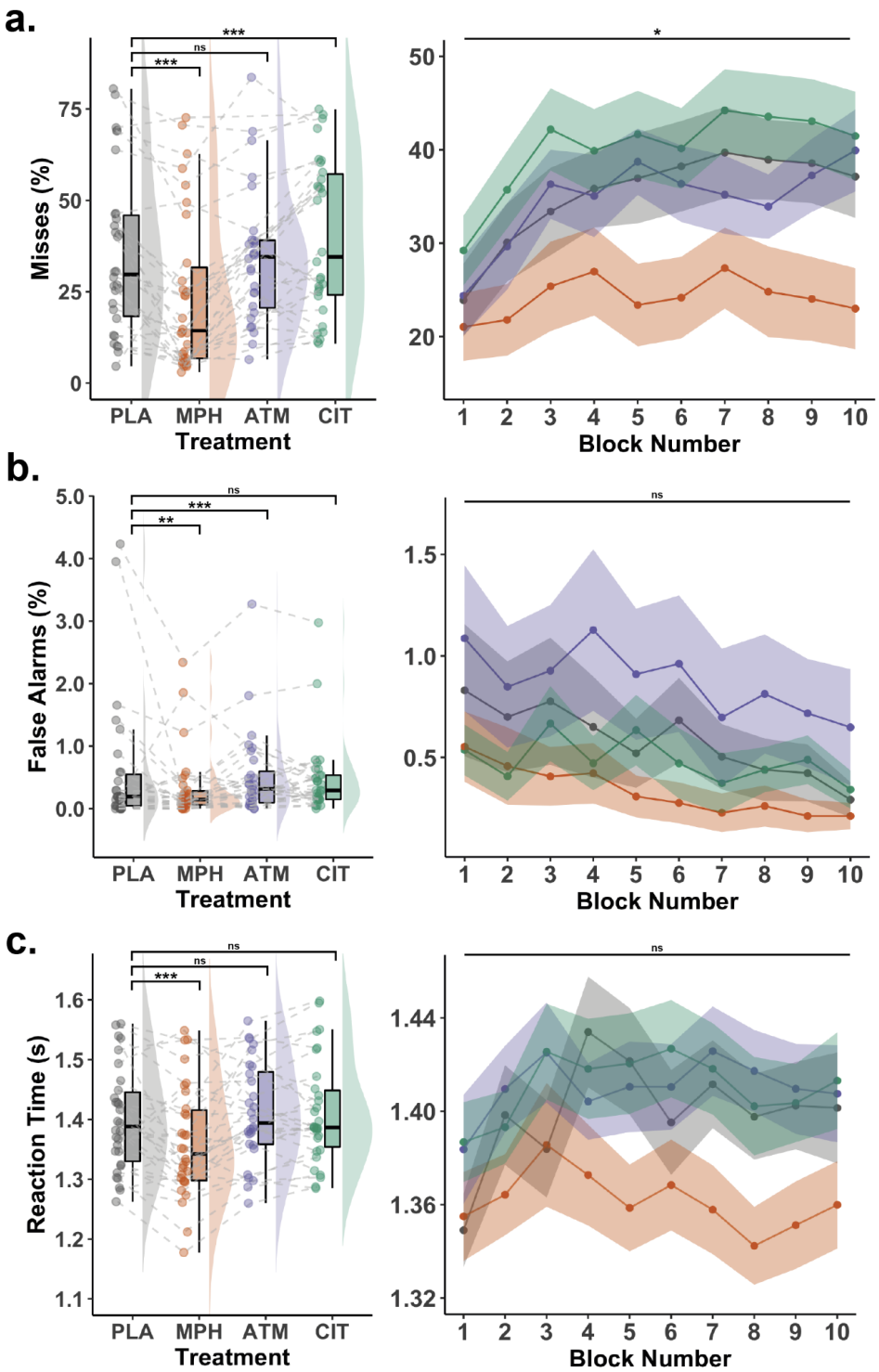

Figure 2. Pharmacological modulations of behavioural performance.
Left panels show the sample and individual averages computed across all CTET blocks (N=10 blocks) for each treatment (PLA: N=32; CIT: N=31; ATM: N=31; and MPH: N=32) in the form of raincloud plots (see Methods). Right panels show the sample averages for each drug treatment and block separately. Panel ***a.*** *shows the percentages of missed target trials (misses), panel* ***b.*** *shows the percentages of false alarms and panel* ***c.*** *shows the averaged reaction times on correctly detected targets. On the left panels, stars denote the significance level (ns: non-*

significant; (*): p < .05; (**): p < .01; (***): p < .001) of the difference between placebo and the three treatments used in this protocol (MPH vs PLA, ATM vs PLA, CIT vs PLA), as determined by linear mixed-effect models. On the right panels, stars denote the significance level (ns: non-significant; (*): p < .05; (**): p < .01; (***): p < .001) of the interaction between block number and drug treatment, as determined by linear mixed-effect models.

Although ATM is also used to reduce ADHD symptoms, in contrast to MPH, it is a non-stimulant. Results indicated that ATM was associated with more false alarms (t = 3.6, $p < .001$) compared with PLA, whereas misses and reaction times did not differ compared with PLA (t = -0.7, $p = .45$ and t = 0.0, $p = .99$ resp.). Thus, ATM decreased performance by increasing impulsive responses (false alarms). However, given the low proportion of false alarms, this did not result in a significant decrement of overall performance compared to placebo, as assessed by d′ (t = -1.7, $p = .09$; Figure S2).

We observed an increase in the proportion of misses under CIT compared with PLA, (t = 4.0, $p < .001$), whereas the proportion of false alarms and the average reaction times did not significantly differ (t = -1.5, $p = .13$ and t = 0.8, $p = .41$, respectively). Thus, contrary to MPH, CIT led to a decrease in sustained attention performance, which was reflected in a decrease of the d′ (t = -2.5, $p = .01$; Figure S2). In addition, whereas ATM resulted in impulsive responses, CIT resulted in the opposite behavioural effect with more misses. Thus, the three pharmacological probes had unique effects on behavioural performance during the CTET, either enhancing or impairing discrete aspects of sustained attention.

Finally, we also examined the effect of time-on-task on behavioural performance and its interaction with the drug treatments. To do so, we fitted linear mixed effect models including block number and treatment as fixed effects, along with their interaction component, and subject identity as a categorical random effect. We tested the significance of the interaction component by comparing this model with the same model minus the interaction component, using the Likelihood Ratio Test. This approach showed that there was an interaction between

322 time and treatment for misses (Likelihood Ratio Test for the model comparison: $\chi^2(3) = 9.15$,
323 $p = 0.03$). This interaction was driven by MPH, which stabilised performance and prevented
324 the increase of misses with time-on-task (Figure 2a). CIT, on the other hand, resulted in a
325 constant increase in misses throughout the task compared to placebo. There was no interaction
326 between time and treatment for false alarms or reaction times ($\chi^2(3) = 2.38$, $p = 0.50$ and
327 $\chi^2(3) = 4.34$, $p = 0.23$, respectively). This analysis confirmed the opposing effects of MPH and
328 CIT on attentional lapses across time.

329 **EEG indexes of visual processing: Event-Related Potentials (ERPs) and Steady-State**
330 **Visual Evoked Potentials (SSVEPs)**

331 To further understand the impact of pharmacological treatment on the physiology of
332 sustained attention, we first focused on two EEG indices of visual processing: Event-related
333 potentials (ERPs) (Figure 3) and steady state visual evoked responses (SSVEPs) (Figure 4).
334 Comparing the ERPs associated with the offset of the Target and non-Target trials revealed a
335 strong P3 effect (Figure 3a), a larger positivity for Target trials, starting at stimulus offset and
336 maximal over parietal electrodes (Figure 3b). We thus extracted the amplitude of this P3
337 component and compared it across drug treatments using a cluster-permutation approach (see
338 Methods). This analysis revealed an increase of the P3 amplitude following MPH
339 administration compared to PLA (Figure 3c), in line with previous findings on this same dataset
340 (Dockree et al., 2017). Interestingly, now examining the impact of ATM and CIT as well, the
341 amplitude of the P3 was not significantly impacted by the administration of these drugs
342 compared with PLA (Figure 3c).

343 The rapid flickering of the visual checkerboard stimuli generated a SSVEP, allowing
344 us to examine the impact of drug treatment on an EEG index of visual processing. We observed
345 a clear peak at the flicker frequency of checkerboard (25 Hz) in the power spectrum (Figure 4a

346 showing the signal-to-noise-ratio (SNR) or power at each frequency bin normalised by
347 neighbouring bins, see Methods). We thus focused on the SNR at 25Hz and compared the
348 strength of this entrainment for each electrode across drug treatments (Figure 4b-c). This
349 analysis revealed an increase for MPH compared to PLA, maximal over central electrodes
350 (Figure 4c). Neither ATM nor CIT significantly modulated the strength of SSVEPs compared
351 to PLA (Figure 4c).

352

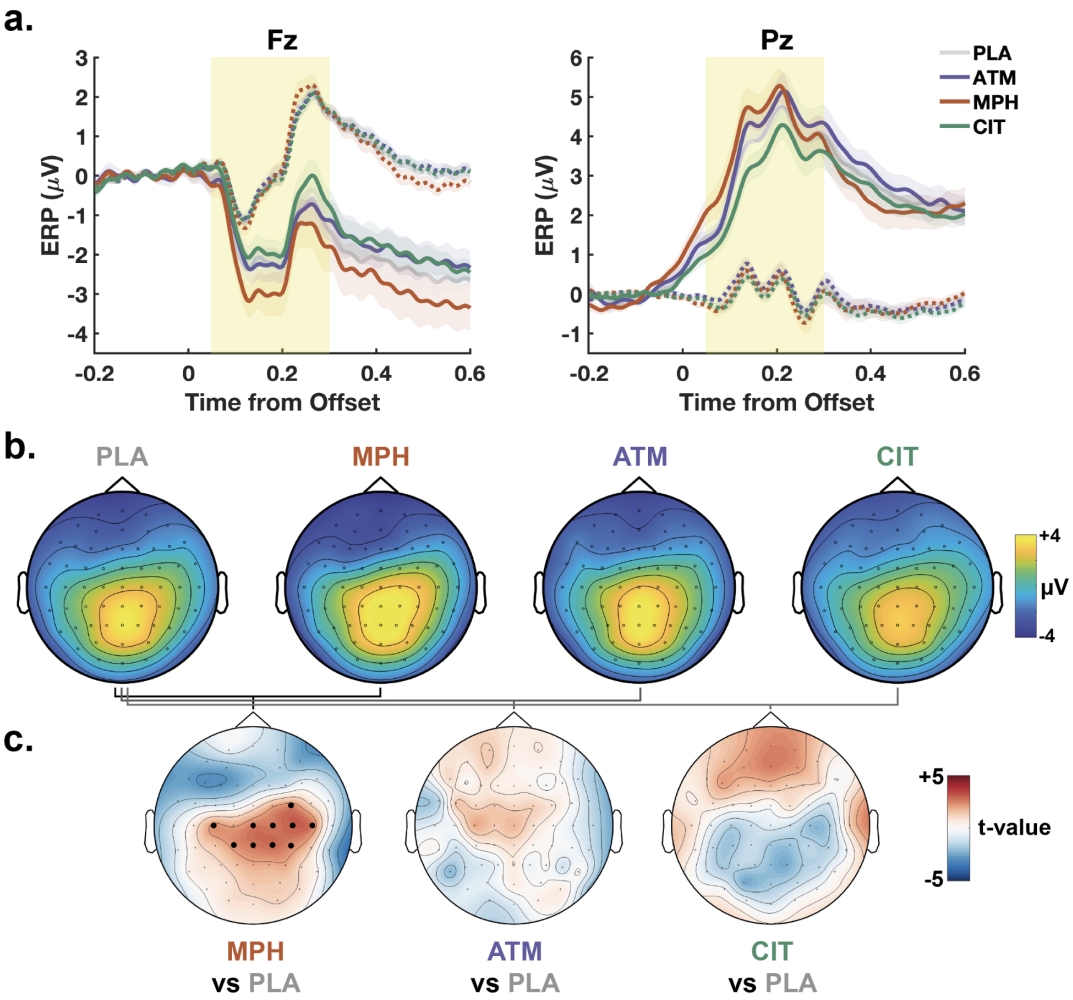

Figure 3. Event-related potentials.
a. *Event-Related Potentials (ERPs) locked on stimulus offset for Target (continuous lines) and non-Target (dashed lines) trials and split by drug treatment (PLA: grey, MPH: orange, ATM: purple, CIT: green). ERPs are averaged across participants (PLA: N=32; CIT: N=31; ATM: N=31; and MPH: N=32). ERPs computed on two electrodes are shown: Fz (Frontal, left) and Pz (parietal, right). Coloured lines show the sample average and coloured areas the standard error of the mean. The yellow area ([0, 0.3]s post-offset window) shows the interval of the archetypal P3 used to compute the P3 amplitude (see Methods).* ***b.*** *Topographical maps of the P3 amplitude (difference of the ERP amplitude between Target and non-Target trials and average on a [0, 0.3]s window) for each drug treatment.* ***c.*** *Topographical maps of the statistical differences in P3 amplitude between MPH and PLA (left), ATM and PLA (middle) and CIT and PLA (right). The t-values obtained with paired t-tests for each electrode are shown. Significant clusters of electrodes ($p_{cluster}$<.05) are shown with black dots (cluster-permutation approach, see Methods). A significant cluster was found only for MPH.*

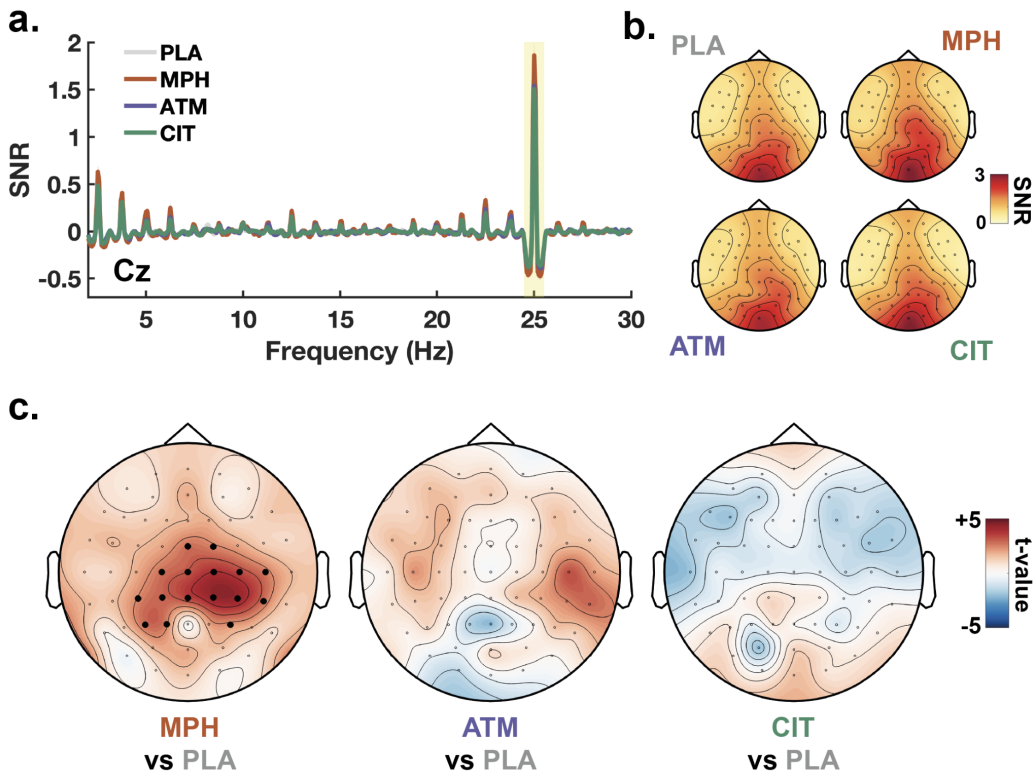

Figure 4. Steady-State Visual Evoked Potentials.
Visual stimuli were flashed at a 25Hz rate on the screen, entraining neural activity at the same frequency (frequency tagging) and generating Steady-State Visual Evoked Potentials SSVEP). This frequency tagging can be observed when computing the power spectrum of the EEG signal and extracting the signal-to-noise ratio (SNR) of the frequency tag (see Methods). ***a.*** *SNR by frequency and drug treatment, computed for electrode Cz and across participants (PLA: N=32; CIT: N=31; ATM: N=31; and MPH: N=32). A clear peak at 25 Hz (highlighted in yellow) is present for all treatments (PLA: grey, MPH: orange, ATM: purple, CIT: green).* ***b.*** *Topographical maps for the SNR at 25 Hz for each drug treatment.* ***c.*** *Topographical maps of the statistical differences in 25 Hz SNR between MPH and PLA (left), ATM and PLA (middle) and CIT and PLA (right). The t-values obtained with paired t-tests for each electrode are shown. Significant clusters of electrodes ($p_{cluster}$<.05) are shown with black dots (cluster-permutation approach, see Methods). A significant cluster was found only for MPH.*

EEG indexes of arousal: Alpha Power and Sleep-Like Slow Waves

To better understand the impact of the drug manipulations on physiological arousal, we examined a classical marker of arousal - alpha power. Inspection of the EEG power spectrum revealed a bump, or deviation from the 1/f trend, in the alpha frequency band (8-11 Hz; Figure 5a). We thus extracted the average power in this band and compared this alpha power across treatments at the electrode level (Figure 5b). A cluster permutation analysis revealed that MPH was associated with reduced levels of alpha power in comparison to PLA, consistent with previous reports (Dockree et al., 2017; Janssen et al., 2016) and the idea that alpha desynchronisation is associated with improved attention. However, no differences were observed for ATM and CIT compared with PLA (Figure 5c).

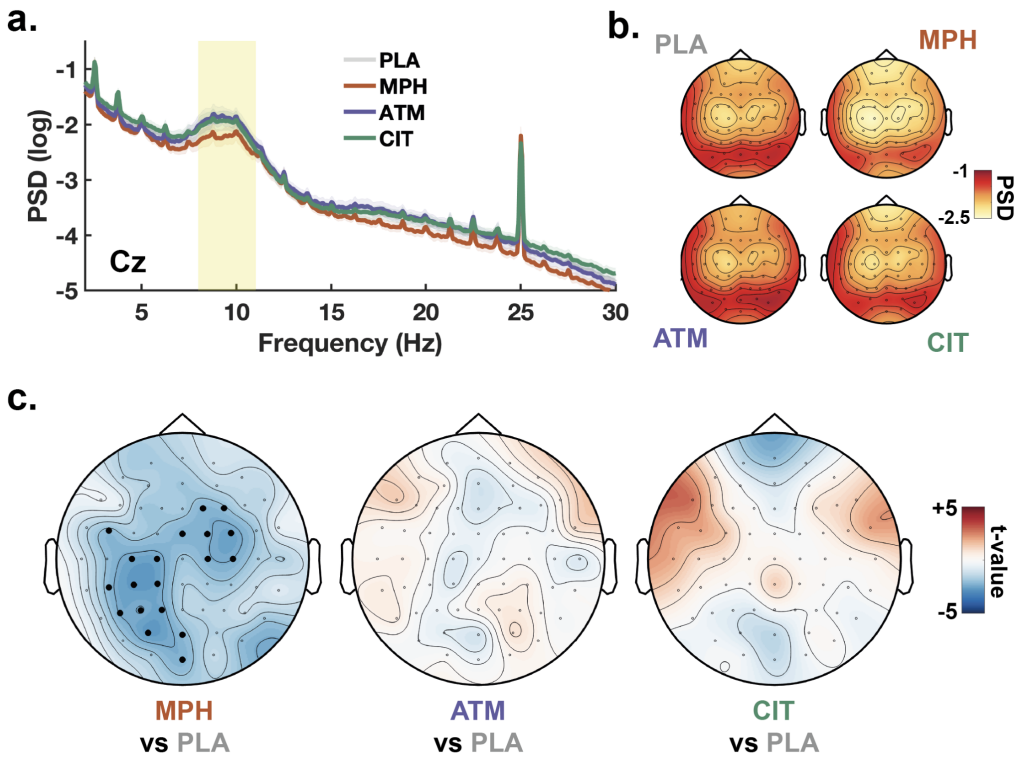

Figure 5. Power of alpha oscillations.
We computed the Power Spectral Density (PSD) to analyse the impact of treatments on alpha oscillations, a common marker of physiological arousal. The power of alpha oscillations was obtained by averaging the log power of the PSD on a [8, 11] Hz window and for each electrode, participant and drug treatment (PLA: N=32; CIT: N=31; ATM: N=31; and MPH: N=32). ***a.***

Average PSD for electrode Cz and for each drug treatment (PLA: grey, MPH: orange, ATM: purple, CIT: green). The alpha power window is highlighted in yellow. ***b.*** *Topographical maps of alpha power for each drug treatment.* ***c.*** *Topographical maps of the statistical differences in alpha power between MPH and PLA (left), ATM and PLA (middle) and CIT and PLA (right). The t-values obtained with paired t-tests for each electrode are shown. Significant clusters of electrodes ($p_{cluster}$<.05) are shown with black dots (cluster-permutation approach, see Methods). A significant cluster was found only for MPH.*

Since only MPH demonstrated effects compared with PLA for the different EEG indices explored thus far (ERPs, SSVEPs and alpha power), these EEG markers are unable to account for the detrimental effects of CIT or ATM on behaviour (Figure 2). In addition, alpha power has a complex relationship with arousal, decreasing both when arousal increases and when individuals approach sleep. We therefore extracted another emerging EEG marker of low arousal, sleep-like slow waves, which has been proposed to index the transition of local networks toward sleep (Andrillon et al., 2019). We applied established algorithms to extract the number of sleep-like slow waves across electrodes and drug treatments (see Methods).

We compared the density of sleep-like slow waves (averaged across all electrodes) across sessions by fitting a linear fixed effect model comprising a fixed categorical effect of drug treatment and a random categorical effect of subject identity. We then compared this model with a model with only subject identity as a random effect (see Methods). A likelihood ratio test revealed that drug treatment had a significant effect on the density of sleep-like slow waves ($\chi^2(3) = 32.79$, $p < .001$). Examining the winning model revealed that this modulation was driven by an increase in slow-wave density for CIT compared to PLA ($t = 5.13$, $p < .001$; Figure 6a). No significant differences were observed for MPH and ATM ($t = 0.19$, $p = .85$ and $t = 1.54$, $p = .12$, resp.). We then explored the interaction between block number and treatment by comparing a model including treatment and experimental block as fixed effects, with a model including both fixed effects and their interaction component. A likelihood ratio test did not reveal a significant interaction between block number and treatment ($\chi^2(3) = 1.15$, $p = .77$,

Figure 6b). Rather, CIT was associated with more slow waves throughout the task, independent of any time-on-task effects. Finally, we examined topographical differences by extracting slow-wave density across electrodes and comparing it across treatments using linear mixed effects models with a single fixed effect of treatment (see Methods). A cluster-permutation analysis revealed a widespread increase in slow-wave density for CIT but no significant clusters for MPH and ATM (Figure 6c).

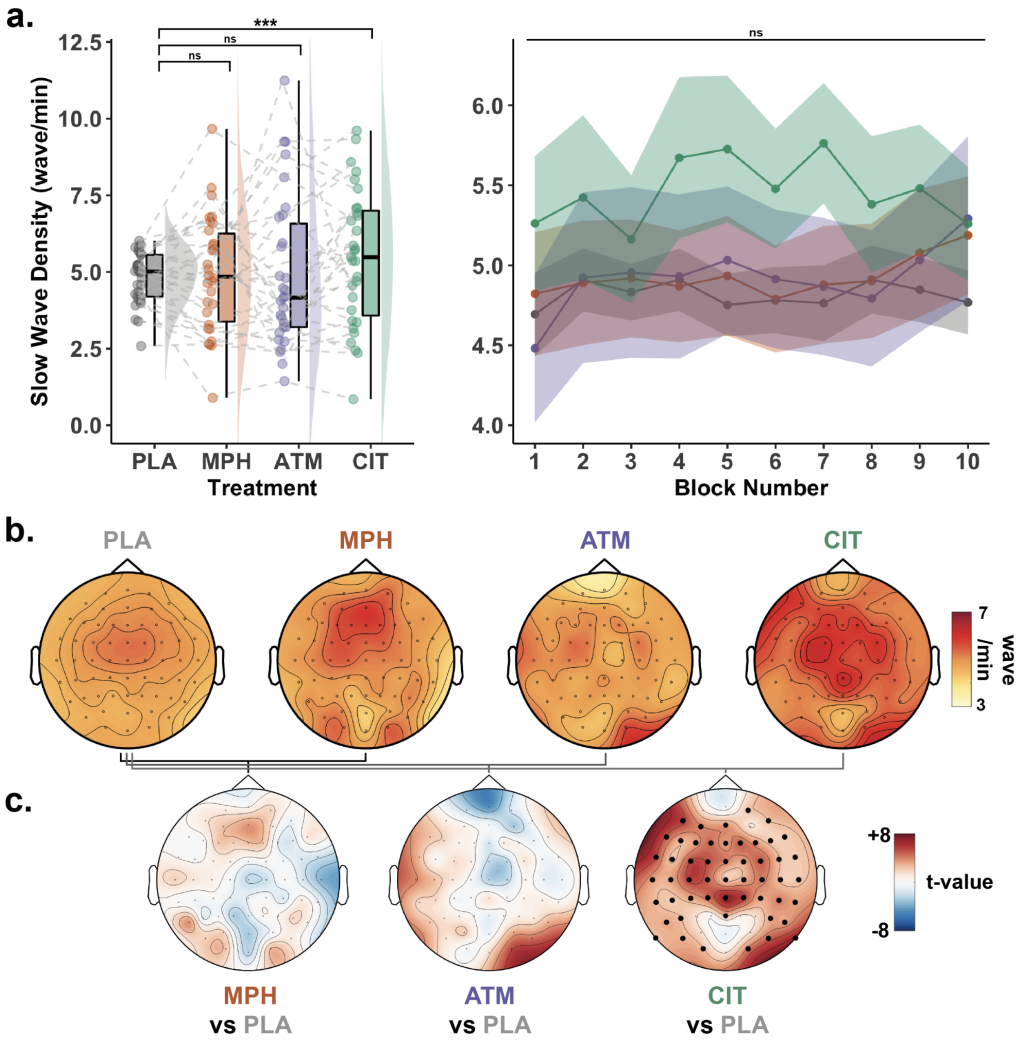

Figure 6. Sleep-like Slow Waves.
a. *Slow-wave density (wave/min averaged across all electrodes) per treatment. The raincloud plot for each drug treatment (PLA: grey (N=32), MPH: orange (N=32), ATM: purple (N=31), CIT: green (N=31)) is shown in the left panel. Stars denote the significance level (ns: non-significant; (*): $p < .05$; (**): $p < .01$; (***): $p < .001$) of the difference between placebo and the three treatments used in this protocol (MPH vs PLA, ATM vs PLA, CIT vs PLA), as determined by linear mixed-effect models. In the right panel, slow-wave density split by*

treatment and block (N=10 blocks) showing the sample average (circle) and standard-error of the mean (coloured areas) across participants is shown. A non-significant interaction (ns) between block number and drug treatment was found, as determined by linear mixed-effect models (see Methods). ***b.*** *Topographical maps of slow-wave density for each drug treatment.* ***c.*** *Topographical maps of the statistical differences in slow-wave density between MPH and PLA (left), ATM and PLA (middle) and CIT and PLA (right). The t-values obtained with mixed-effect models for each electrode are shown (see Methods). Significant clusters of electrodes ($p_{cluster}<.05$) are shown with black dots (cluster-permutation approach, see Methods). A significant cluster was found only for CIT.*

Predicting behavioural errors with EEG indices of arousal

Given that alpha power decreased following the administration of MPH (Figure 5c) and slow waves increased following the administration of CIT (Figure 6c), and since these two treatments also showed the strongest modulations of behavioural performance (Figure 2), we examined whether the amount of alpha power or the density of slow waves at the sensor level could predict behavioural performance, irrespective of drug treatment, and the spatial distributions of these effects. To do so, we fitted linear mixed effect models for each scalp electrode using the proportion of misses, false alarms, or the average reaction times as predicted variables, and either slow waves or alpha power as a single fixed effect. In all these models, subject identity was fitted as a random categorical effect. We then used a cluster permutation approach to identify clusters of electrodes for which alpha power or slow waves significantly predicted behavioural variables (Figure 7, bottom).

This analysis revealed that an increase in alpha power was predictive of an increase in misses in all electrodes. An increase in alpha power was also predictive of a slowing of responses over centro-parietal electrodes. Finally, an increase in alpha power was negatively associated with false alarms in frontal, left temporal and occipital electrodes. In all three of these cases, topographical maps were homogeneous in the sense that, across all electrodes, the association between alpha power and behavioural variables was always in the same direction (positive for misses and reaction times, negative for false alarms).

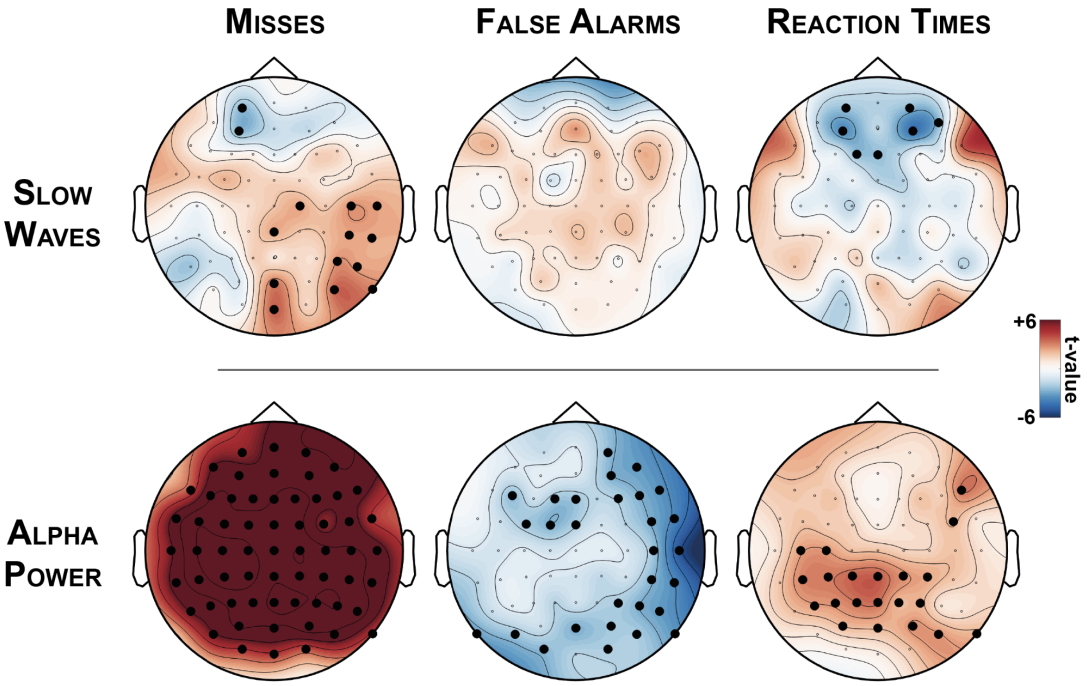

Figure 7. Predicting behavioural errors with slow waves and alpha power.

We used slow waves (top row) and alpha power (bottom row), two complementary markers of physiological arousal, to predict behavioural variables: misses (left), false alarms (middle) and reaction times (right). For each predictor (slow waves or alpha power) and each behavioural variable (misses, false alarms, and reaction times), we fitted mixed-effect models at the electrode level (see Methods). The t-values derived from these models and estimating the influence of the predictor on the behavioural variable of interest are shown as topographical maps. Significant clusters of electrodes ($p_{cluster}<.05$) are shown with black dots (cluster-permutation approach, see Methods). Both alpha power and slow waves predict behavioural errors, but slow waves do so in a region-specific fashion.

Slow waves, on the other hand, had contrasting effects (Figure 7, top). An increase in temporo-occipital slow waves was predictive of more misses but an increase of frontal slow waves was associated with a reduction of missed targets. In addition, an increase in slow waves over frontal electrodes was associated with faster responses and, although there were no significant clusters over temporal or occipital electrodes, these electrodes showed a reversal in the direction of these effects (positive correlation between slow waves and reaction times). These effects suggest that slow waves can have opposite associations with behavioural errors depending on the spatial location of their occurrence.

496 # Discussion

497 This study aimed to determine the relationship between physiological arousal and
498 sustained attention by manipulating key neuromodulators (noradrenaline, dopamine, and
499 serotonin) via the administration of three different drugs (MPH, ATM, and CIT) in a four-arm,
500 randomised, placebo-controlled trial (Figure 1).

501 **Sustained attention is fine-tuned by neuromodulators**

502 Although sustained attention performance classically decrements with time-on-task
503 (Parasuraman, 1979), we found that MPH decreased misses and false alarms, and led to faster
504 responses compared to placebo (Figure 2). These effects were paralleled by stable subjective
505 reports of sleepiness (Figure S1), meaning that participants did not experience the classical
506 build-up of fatigue with time-on-task. These results replicate previous findings in this dataset
507 (Dockree et al., 2017) and others within the literature (Bedard et al., 2015; Lufi et al., 2015;
508 Nandam et al., 2011; Solanto, 1998; Spencer et al., 2009). The beneficial effect of MPH could
509 stem from its combined effect on both dopamine and noradrenaline, neuromodulators involved
510 in cortical activation (Jones, 2005) and motivation (Robbins, 1997). More specifically, MPH
511 increases noradrenaline and dopamine levels in the prefrontal cortex (Berridge et al., 2006) and
512 the striatum (Volkow et al., 2012), brain regions involved in the execution and monitoring of
513 action (Arnsten and Li, 2005) and action selection and motivation (Liljeholm and O'Doherty,
514 2012) respectively.

515 Our results for ATM however show that increasing the concentrations of noradrenaline
516 and dopamine does not necessarily lead to behavioural improvements. Indeed, ATM led to
517 similar levels of sleepiness (Figure S1, BF_{01}=5.8), misses and reaction times (Figure 2, BF_{01}>3)
518 and an increase in false alarms (Figure 2), although this did not result in an overall decrease in
519 d' (Figure S2, BF_{01}=1.9). This pattern of results suggests that participants tended to become

impulsive under ATM, without making them more attentive to the target trials. This difference in results for ATM and MPH is somewhat surprising given that both target noradrenaline and dopamine. This inverted U-shaped pattern could stem from the particular responsiveness of the noradrenaline system (Graf et al., 2011; Ross and Van Bockstaele, 2021). Tailored administration of ATM doses could therefore have resulted in improvements in task performance, although this was not achieved with the fixed acute dose used here. Alternatively, the failure of ATM to improve performance in contrast with MPH could be due to the fact that ATM impacts the dorsolateral prefrontal cortex, in contrast to the broader effects of MPH on thalamo-cortical networks (Bymaster, 2002; Farr et al., 2014; Kowalczyk et al., 2019). Indeed, although MPH targets mostly prefrontal cortices, it has a more widespread cortical effect than ATM and, in particular, increases the concentration of dopamine in the striatum (Volkow et al., 2012). Thus, our results imply that increasing noradrenaline and dopamine may be more likely to improve performance when released across cortical and subcortical areas.

Finally, the administration of CIT led to a different pattern of results with participants missing more targets, without a slowing down of reaction times or an increase in false alarms (Figure 2, $BF_{01}>3$ for reaction times and false alarms). The increased misses led to a significant decrease in behavioural performance (d') compared to placebo (Figure S2) and can be interpreted as participants being more sluggish (which contrasts with the impulsivity following ATM administration). This interpretation is in line with previous work on another selective serotonin reuptake inhibitor (SSRI), paroxetine, which resulted in an increase in missed targets and reaction times (Schmitt et al., 2002). Our results may also provide indirect support for the theory that serotonin inhibits the activity of the noradrenergic and dopaminergic systems, causing impairments in behaviour (Robbins, 1997; Wingen et al., 2008).

Overall, these results show that optimal performance on a sustained attention task needs to be achieved by balancing activation and inhibition, impulsivity and sluggishness. Of course,

545 this optimal balance is achieved through the synergetic effects of various neuromodulators and
546 although the medications administered to participants were aimed at specific neuromodulatory
547 systems, additional downstream effects and interactions between these systems may play a
548 role.

549 **Methylphenidate boosts visual processing**

550 We investigated drug-induced changes in visual processing through two
551 complementary EEG indices: ERPs and SSVEPs. ERPs are a classical approach to decompose
552 and quantify the sub-processes involved in a particular cognitive task (Kappenman and Luck,
553 2011). It allows one to isolate components such as the P3, which has been associated with the
554 detection of rare, task-relevant events (Polich, 2007) and which is strongly elicited by the
555 CTET (Figure 3a). In agreement with a previous report on the same dataset (Dockree et al.,
556 2017), the administration of MPH robustly enhanced the amplitude of the P3 over central
557 electrodes (Figure 3b-c). Examining SSVEPs confirmed an enhancement of visual processing
558 with MPH (Figure 4b-c). This increase was maximal over central electrodes and overlapped
559 with the increase of the P3. This result differs this time from the previous report on the same
560 dataset (Dockree et al., 2017), which can be explained by the fact that the effect is observed
561 here over centro-parietal electrodes and not over occipital electrodes, which show the strongest
562 SSVEP and which were investigated in (Dockree et al., 2017). Finally, we report here that
563 ATM and CIT had no significant effect on the P3 or SSVEP amplitude.

564 Overall, these results indicate that MPH boosted visual processing, in accordance with
565 the improvement in behavioural performance. These results are consistent with previous
566 findings showing an enhancement of visual responses with increases of noradrenaline
567 (Gelbard-Sagiv et al., 2018). This enhancement could result from the improvement of neuronal
568 gain and signal-to-noise ratios with the increase in noradrenaline and dopamine levels (Thiele

569 and Bellgrove, 2018) . However, the fact that the effect on the frequency tag was maximal over
570 central electrodes, that is, away from the primary visual cortex generating the SSVEP, suggests
571 that higher-level, cognitive processes are at play. An increase in noradrenaline could have
572 increased participants' attentional focus, resulting in both stronger SSVEPs and P3 in the
573 cortical network tasked to detect target trials. An increase in dopamine could also heighten
574 motivation (Ranjbar-Slamloo and Fazlali, 2020; Thiele and Bellgrove, 2018) and lead to
575 similar behavioural improvements. Importantly, no significant modulation was observed for
576 the P3 or SSVEP for ATM and CIT, despite the impact of these drugs on performance. This
577 suggests that the detrimental effect of ATM on false alarms and of CIT on misses is unlikely
578 to result only from a degradation of the integration of visual information.

579 **EEG markers of sleepiness are linked to changes in sustained attention**

580 To better understand the neural mechanisms underlying the pharmacological effects on
581 behaviour, we examined how the different treatments impacted neural indices of arousal. We
582 first focused on alpha oscillations, a resting activity linked to the (active or passive) decrease
583 in visual processing over early visual cortices and which has been tied to modulations of
584 arousal. Here, we observed that alpha power was reduced following the administration of MPH.
585 This is in line with the effect of noradrenaline on the promotion of wakefulness (Lee and Dan,
586 2012; Robbins, 1997; Sara and Bouret, 2012) and the use of MPH in the treatment of
587 narcolepsy (Mignot, 2012). A positive effect of MPH on arousal through the increase in
588 noradrenaline is also in line with the stabilisation of subjective sleepiness following MPH
589 administration (Figure S1) and the positive behavioural and electrophysiological effects of
590 increased noradrenaline reported elsewhere (Gelbard-Sagiv et al., 2018).

591 However, the relationship between alpha power and vigilance is not monotonic and,
592 when individuals near sleep, alpha power also decreases. Alpha oscillations are thus a rather

593 ambiguous index of fatigue since a desynchronization of alpha oscillations can be associated
594 with both an increase and a decrease in alertness. To circumvent this limitation, we focused on
595 another, emerging index of fatigue: sleep-like slow waves (Andrillon et al., 2019; D'Ambrosio
596 et al., 2019). Indeed, recent research has shown that extended wakefulness and/or engagement
597 in a given task-set is associated with an increase in patterns of EEG activity reminiscent of
598 sleep slow waves (Bernardi et al., 2015; Hung et al., 2013; Vyazovskiy et al., 2011). These so-
599 called "local sleep" intrusions may result from a gradual transition of cortical activity towards
600 a bistable dynamic (Vyazovskiy et al., 2011). This bistable dynamic is characterised by the
601 occurrence of "down-states" in which neuronal assemblies are silent. These neuronal lapses,
602 when occurring during wakefulness, could impair the cognitive processes performed by the
603 impacted neuronal networks, leading to attentional lapses and errors (Andrillon et al., 2019).

604 To determine if sleep-like slow waves could partly explain the behavioural effects of
605 medications, we isolated these slow waves from the ongoing EEG activity while participants
606 performed the CTET. These detected slow waves had a spatio-temporal profile in line with
607 previous wake and sleep studies (Andrillon et al., 2021). Furthermore, we observed an increase
608 in the number of these sleep-like slow waves following the administration of CIT, a drug that
609 can be associated with sleepiness although it is less sedative than other classes of
610 antidepressants (Milne and Goa, 1991). Such an increase is also in line with recent findings
611 linking serotonin with the build-up of sleep pressure in wakefulness (Jouvet, 1999; Oikonomou
612 et al., 2019). Thus, an increase in serotonin levels through the administration of CIT could have
613 favoured the occurrence of these slow waves by shifting cortical dynamics towards bistability.
614 The fact that this increase was observed in nearly all scalp electrodes suggests a systemic
615 impact of serotonin.

616

617 **Indexes of arousal can predict behavioural performance**

618 A key aspect of the local sleep framework is that slow waves are predicted to be
619 mechanistically linked with the behavioural consequences of fatigue (Andrillon et al., 2019, p.
620 201). This is supported by their use-dependent increase in sleep deprivation studies as well as
621 by their region-specific consequences. Even in awake, non-sleep deprived individuals, the
622 cognitive consequences of slow waves depend on the location of these slow waves, with frontal
623 slow waves associated with impulsivity and posterior slow waves associated with sluggishness
624 (Andrillon et al., 2021). These consequences can be linked back to the respective involvement
625 of frontal cortices in executive control and parietal cortices in sensory integration and response
626 preparation. Thus, one can expect slow waves to be (1) predictive of behavioural errors (2) in
627 a region-specific fashion. Crucially, this is in contrast with alpha oscillations, which represent
628 a sensor and not an effector of the transition toward sleep and low levels of alertness.

629 Our present findings support these hypotheses as alpha power was predictive of only a
630 certain type of behavioural error (sluggishness) and in a homogeneous fashion (Figure 7): all
631 significant electrodes were positively associated with misses and slower reaction times, and
632 negatively associated with false alarms. Importantly, electrodes outside these clusters always
633 showed the same direction of effect compared with the electrodes within the clusters,
634 reinforcing the homogeneity of these statistical maps. In contrast, the relationship between slow
635 waves and behavioural errors showed regional specificities and slow waves accounted for both
636 more misses and shorter reaction times (Figure 7). In particular, a small cluster of frontal
637 electrodes showed a negative relationship between misses and reaction times, in contrast with
638 posterior electrodes which showed the reverse relationship with misses. Thus, according to our
639 hypotheses, a unique marker of hypo-arousal could account for the heterogeneous fingerprint
640 of attention failures and their combination of sluggishness and impulsivity. Indeed, the
641 paradoxical association between frontal slow waves and an improvement in behaviour could

642 be explained by a decrease of inhibition (through impairment of frontal cortices), which would
643 facilitate fast (but potentially impulsive) responses. A similar antero-posterior contrast has been
644 found in regards to subjective experience (larger slow waves in frontal electrodes being
645 associated with more mind wandering and larger slow waves in posterior electrodes being
646 associated with more mind blanking) in healthy well-rested, un-medicated individuals
647 (Andrillon et al., 2021). However, we did not observe a cluster of electrodes with a significant
648 correlation between the occurrence of slow-waves and false alarms. This could be related to
649 the rare occurrence of both false alarms (<1%) and slow waves (<0.1 wave/second).

650

651 **Conclusion**

652 Sustained attention is fine-tuned by a combination of neuromodulators, possibly
653 through the maintenance of an optimal level of physiological arousal and the balance of
654 excitation and inhibition. The effect of MPH suggests that promoting arousal can lead to
655 improved visual processing and behaviour through the combined effect of dopamine and
656 noradrenaline. We also found that decreasing arousal through an increase in serotonin levels
657 led to poorer behaviour in terms of increased misses. Importantly, this behavioural impairment
658 seems associated with a state of hypo-arousal, characterised by the intrusion of sleep-like slow
659 waves in wakefulness. These intrusions seem to result in local, region-specific consequences
660 on behaviour and could represent a simple, unitary mechanism accounting for the various
661 behavioural outcomes of inattention. This research paves the way for future studies seeking to
662 examine the link between arousal and attention in clinical populations. These results also
663 reinforce the notion that the pattern of behavioural impairments observed in disorders such as
664 ADHD, might stem from a dysregulation of arousal (Owens, 2005).

Materials and methods

We re-analysed data from a previously published study (Dockree et al., 2017), adding new analyses and focusing on two additional drugs. This re-analysis was approved by the Monash University Human Research Ethics Committee (Project Number: 4663).

Participants

Forty (N=40) healthy participants were recruited in accordance with the ethical guidelines of the University of Queensland (Project Number: 2008000463). Participants were all right-handed Caucasian males, aged 18 to 45 years (μ = 24.3 years, σ = 5.6 years) who were non-smokers, had no history of neuropsychiatric disorder, and were not under the influence of recreational drugs or psychoactive medication at the time of the study. They were screened for psychiatric disorders using the Mini-International Neuropsychiatric Interview Screen (Sheehan et al., 1998) and completed the Conners' Adult ADHD Rating Scales (Conners et al., 1999). The mean for the total ADHD symptoms in the group was 49.73 (σ = 11.89), below the threshold for ADHD diagnosis (threshold: 65). Eight (N=8) participants were discarded from our analyses (contraindications to the study medications: 4; data loss: 1; technical issues: 3) leaving 32 participants for our analyses. 30/32 participants completed all four versions and the remaining two had one missing session (but completed the placebo session: PLA: N=32; CIT: N=31; ATM: N=31; and MPH: N=32).

Procedure and Pharmacological Intervention

A randomised, double-blinded, placebo-controlled paradigm was used in which participants partook in four different experimental sessions. Participants were required to fast for at least one hour prior to each session. They were randomly administered a different drug, 90 minutes prior to the commencement of cognitive testing (Figure 1A). These drugs included ATM (60 mg), MPH (30 mg), CIT (30 mg) or a placebo (dextrose). ATM inhibits the reuptake

689 of noradrenaline and dopamine, and thus, is commonly used to increase noradrenaline and
690 dopamine levels (Bedard et al., 2015; Bymaster, 2002; Ding et al., 2014). MPH inhibits
691 noradrenaline and dopamine transporters, resulting in an increase in cortical noradrenaline and
692 striatal dopamine levels (Farr et al., 2014; Kowalczyk et al., 2019; Volkow et al., 2012). CIT,
693 an SSRI, increases serotonin levels (McKie et al., 2005). Doses were selected according to the
694 reported effects on cognition from past studies (Aron et al., 2003; Graf et al., 2011; Nandam et
695 al., 2014). To avoid drug interactions, each session took place at least a week apart to allow the
696 washout of drugs. Sessions took place at the same time of the day and same day of the week
697 for each participant.

698 After ingesting the medication, participants waited for 60 minutes. They were then
699 equipped with a high-density electroencephalographic cap (64 active electrodes cap,
700 ActiveTwo BioSemi system), which took approximately 30 minutes. This ensured a 90 minute
701 delay between medication administration and the commencement of testing, allowing the three
702 treatments to reach peak plasma levels (Chamberlain et al., 2009; Kowalczyk et al., 2019;
703 Nandam et al., 2014; Sauer et al., 2005). EEG recording lasted for approximately 90 minutes
704 whilst the participants completed two tasks, the order of which was counterbalanced: a
705 Continuous Temporal Expectancy Task (CTET) (Connell et al., 2009; Dockree et al., 2017)
706 and a standard Eriksen flanker task (Barnes et al., 2014). We focused here on the CTET data.

707 For each session, participants first completed a visual analogue scale (VAS) (Bond and
708 Lader, 1974) to report their sleepiness, calmness and contentedness (Norris, 1971) across three
709 intervals: immediately prior to drug administration, prior to cognitive testing (+90 minutes),
710 and after cognitive testing (+180 minutes). We analysed here only the results from the
711 sleepiness scale.

712

713 **Continuous Temporal Expectancy Task (CTET)**

714 The CTET measures sustained attention. Participants were instructed to monitor a
715 centrally presented patterned stimuli with a grey background (Figure 1B). The stimuli consisted
716 of a square with an 8 cm^2 dimension. This was further divided into a 10 by 10 grid of squares,
717 each diagonally split in half into white and black. Each time the frame changed, the stimuli
718 randomly altered its orientation by 90° in a clockwise or counter-clockwise direction,
719 producing four different arrangements. A white cross was present at the centre of the frame
720 that participants were instructed to fixate on to limit eye movements. Each pattern was
721 presented for a duration of either 800 milliseconds (standard stimuli) or 1120 milliseconds
722 (target stimuli). Between two target stimuli, 7 to 15 non-target stimuli were pseudo-randomly
723 presented. This equated to 5.6 to 12 seconds between each target presentation. Thus, this task
724 required participants to continuously concentrate on the stream of visual information presented
725 to them. In addition to the transition between patterns, each pattern flickered at 25 Hz during
726 the stimulus presentation window. This allowed the generation of steady state visually evoked
727 potentials (SSVEP). Participants were required to monitor the duration of each stimulus,
728 pressing a button for each target stimulus detected. Prior to starting the CTET, participants had
729 to practice the task until their performance level reached 100%. They then completed 10
730 experimental blocks, with each block containing 225 frames, 18 to 22 target stimuli
731 presentations and lasting approximately 3 minutes. Participants were given a one-minute break
732 in between blocks.

733 **Behavioural Data**

734 For the CTET, we computed the proportion of missed targets (target trials which were not
735 associated with a response) and false alarms (non-target trials associated with a response). We
736 also computed the reaction times of correctly detected target trials. A target stimulus was

737 considered missed if a response was not registered from 800ms after target onset and 1600ms
738 after the target offset (minimal reaction time: 0.8s; maximal reaction time: 2.72s). A false alarm
739 was defined by the presence of a response to a non-target stimulus without any target stimulus
740 in the two preceding trials. Reaction times for target trials were computed from the stimulus
741 onset. These behavioural variables were compared across drug treatments (Figure 2).

742 Indexes of participants' performance were extracted for each CTET block as follows:
743 percentage of missed targets, percentage of false alarms and average reaction times for
744 correctly detected targets (in seconds). To integrate the performance on both target and non-
745 target trials in one single variable, we also computed the d' at the block level (Figure S2)
746 following the Signal Detection Theory (Macmillan, 1993).

747 **Electroencephalography**

748 ***Data acquisition.*** EEG data were recorded using 64 active scalp electrodes and an
749 ActiveTwo BioSemi amplifier. EEG was sampled at 1024 Hz. Eye-movements were recorded
750 with pairs of electrodes (electrooculogram, EOG) placed above and below the left eye (vertical
751 eye-movements), and at the outer canthus of each eye (horizontal eye-movements). EEG data
752 were subsequently analysed using the Fieldtrip toolbox (Oostenveld et al., 2011) and custom
753 code.

754 ***Pre-processing of EEG Data.*** Raw EEG data were epoched on a [-0.5, 1.8]s window
755 around stimulus onset. The average voltage computed across the entire epoch was removed
756 and EEG data were lowpass-filtered below 40Hz (Butterworth filter at the 4th order) and notch-
757 filtered at 50Hz using a Discrete Fourier Transform to remove line noise. EEG data were then
758 down-sampled at 256 Hz and baseline corrected ([-0.5, 0]s). These pre-processed data were
759 then visualised to detect faulty electrodes and artefacted trials (based on the signal variance).
760 The former were interpolated using the "weighted" method from Fieldtrip and the latter were

761 discarded. Finally, EEG data were re-referenced to the average of all electrodes and an
762 Independent Component Analysis (ICA) decomposition was performed to visually identify
763 components associated with ocular artefacts (blinks and saccades). These components were
764 removed from the data epoched on trials.

765 In parallel, we also epoched raw EEG data on experimental blocks (from -2s after the
766 onset of the first trial to 1s after the offset of the last trial of the block). Data were demeaned,
767 lowpass-filtered below 40Hz (Butterworth, 4th order), highpass-filtered above 0.1Hz
768 (Butterworth, 4th order) and notch-filtered at 50Hz (Discrete Fourier Transform). Data were
769 then resampled at 256 Hz and baseline corrected ([-0.5, 0]s from block onset). Faulty electrodes
770 detected on trial-epoched data were interpolated and ocular ICA components (obtained from
771 the data epoched on trials) were removed. Prior to ICA removal, EEG data were re-referenced
772 to the average of all electrodes.

773 We used trial-epoched data for the analysis of Event-Related Potentials (ERP) and
774 block-epoched data for the analysis of the Power Spectrum and the detection of Slow Waves.
775 For topographical analyses, peripheral electrodes (Iz, P9 and P10) were removed, resulting in
776 61 electrodes being analysed.

777 ***Event related potentials.*** Event-Related Potentials were extracted for Target and Non-
778 Target trials separately. Data were re-aligned according to stimuli's offset ([-0.2, 0.8]s) in order
779 to take into account the different duration of Target and Non-Target trials. The EEG data were
780 baseline-corrected from -0.2s to 0s prior to the offset. For each participant, the corresponding
781 ERPs were averaged across trials for the different drug treatments. In Figure 3, we show the
782 corresponding ERPs for electrodes Fz and Pz. Based on these ERPs and previous findings
783 (Dockree et al., 2017), we extracted the average amplitude of the P3 potential typically elicited
784 by Target trials (in comparison with non-Target trials). The P3 amplitude was defined as the

difference in amplitude between the ERP associated with Target trials and the ERP associated with non-Target trials averaged on a [0, 0.3]s window post-offset (Figure 3a).

Spectral Analysis. We computed the power spectral density (PSD) of each EEG electrode using data epoched on experimental blocks. This was done using Welch's method with windows of 10s, a 50% overlap between windows and a frequency resolution of 0.1 Hz between 2 and 40 Hz. The PSD was log-transformed (base-10 log) for further analysis. We extracted the alpha power by averaging for each participant, session, block, and electrode the power within the [8, 11] Hz frequency band. This estimation of the strength of alpha oscillation was compared across drug treatments (Figure 5) and used to predict behavioural performance (Figure 7).

We also extracted the strength of the SSVEP frequency tag by computing the signal to noise ratio (SNR) of each frequency compared to its neighbours. This was done to identify sharp peaks in the power spectrum (associated with the frequency tagging), departing from the 1/f trend. In practice, the PSD for each frequency was divided by the average PSD on a [-0.5, -0.1] Hz and [0.5, 0.1] Hz window around this frequency. This ratio was then log-transformed for further analysis (base-10 log). We extracted the SNR at 25 Hz (frequency of the SSVEP) for each participant, session, block, and electrode. This estimation of the strength of the frequency tagging was then compared across drug treatments (Figure 3).

Sleep-like slow waves. The presence of sleep-like slow waves in the EEG was assessed as in Andrillon et al. (2021), based on established algorithms used to detect local sleep in sleep (Riedner et al., 2007). In practice, EEG data re-referenced to the average of the mastoid's electrodes (TP7 and TP9) were bandpass filtered between 1 and 10Hz using a type-2 Chebyshev filter. For each block and electrode, we then centred the filtered signal around 0 by removing the average voltage computed across the entire block. Individual waves were then

809 detected by locating all the negative peaks between two negative zero-crossings, which were
810 respectively defined as the beginning and end of the wave. The positive peak of the wave was
811 defined as the maximum voltage between this beginning and end. For each wave, we computed
812 its duration, frequency, peak-to-peak amplitude, downward slope (from the beginning to the
813 negative peak) and upward slope (from the negative peak to the positive peak). Waves with a
814 frequency above 7Hz (i.e. outside the delta/theta range: [1, 7] Hz), a positive peak above 75µV
815 or within 1s of a high-amplitude event (absolute amplitude >150µV) were discarded.

816 Finally, we focused on large-amplitude slow waves. To do so, we computed the
817 amplitude threshold of the top 10% of the largest waves recorded in the placebo session using
818 their peak-to-peak amplitude. This threshold was computed for each individual and each
819 electrode and was used to define large-amplitude slow waves in all sessions. Thus, the number
820 of slow waves can be compared within-subject, using the placebo session as a reference. We
821 computed the average temporal profile and spatial distribution of these waves (Figure S3) to
822 confirm their resemblance to sleep-like slow waves detected in wakefulness in previous studies
823 as well as typical slow waves detected during sleep. We finally computed the average number
824 of these slow waves per minute for each experimental block of each session (Figure 6).

825 **Statistical Analyses**

826 VAS sleepiness scores were analysed with a two-way repeated measure ANOVA, with
827 time points (t=0, +90, and +180 minutes post-drug administration, Figure 1A) and treatment
828 (MPH, ATM, CIT and PLA) coded as within-subject effects. We discarded two participants
829 who did not have all four experimental sessions from this analysis. The ANOVA was
830 performed with the 'anova_test' function from the 'rstatix' package in R. We then examined
831 separately post-hoc comparisons by time points and within treatments, and corrected the
832 corresponding *p*-values for multiple comparisons using the Bonferroni method.

833 Linear mixed effect models (LMEs) were implemented in R using the 'lme4' package
834 (Bates et al., 2015) to determine the effects of treatments (categorical fixed effect) on several
835 variables of interest: proportion of misses, proportion of false alarms, reaction times on target
836 trials and slow wave density (averaged across all electrodes). These variables were computed
837 for each block of each session. Subject identity was considered a random categorical effect.
838 We report the estimate and *p*-values for the comparison of the different drugs (MPH, ATM and
839 CIT) with the placebo session.

840 When testing the influence of the time spent on the task (Figure 2), we added a fixed
841 effect of block number as well as an interaction component with the effect of neuromodulation.
842 The significance level of the interaction was assessed by comparing the model with and without
843 the interaction component using the R Studio 'anova' function from the 'stat' package. We
844 report the Likelihood Ratio Test outcomes (chi-squared and *p*-values) for these tests.

845 Examining the influence of treatments on alpha power ([8, 11]Hz log-PSD), frequency
846 tagging (SNR at 25Hz) and event-related potentials ([0, 0.3]s ERP amplitude post offset) for
847 each electrode leads to the multiplication of non-independent statistical tests. We used a
848 cluster-permutation approach to mitigate this issue (Maris and Oostenveld, 2007). For each
849 electrode, we computed the *t*-value and *p*-value corresponding to the paired comparison (*t*-test)
850 for the variable of interests (alpha power, frequency tagging and ERPs) along contrasts of
851 interest (MPH vs PLA, ATM vs PLA, and CIT vs PLA). To examine the effect of treatment on
852 slow-wave density at the electrode level, we used a similar approach but using LMEs to
853 consider the non-normal distribution of slow-wave density. *T*-values were derived from the
854 LMEs (with treatments as a categorical fixed effect and subject identity was considered a
855 random categorical effect) for the same contrasts (MPH vs PLA, ATM vs PLA, and CIT vs
856 PLA). Clusters of neighbouring electrodes were defined as electrodes with *p*-values below .05
857 (cluster alpha). Once the clusters were defined, a comparison was performed with permuted

858 datasets (N=1000 permutations) and we used a Monte-Carlo *p*-value threshold of .05 (one-
859 sided test) to identify the significant clusters ($p_{cluster}$). Only clusters with at least 2 electrodes
860 were retained and shown in Figure 3-7.

861 When analysing the effect of slow-wave density and alpha power on behaviour
862 (proportion of misses, proportion of false alarms, and reaction times on target trials), we
863 implemented linear mixed effect models (LMEs). Slow-wave density or alpha power were used
864 as a fixed effect and subject identity was coded as a categorical random effect. We fitted one
865 model per electrode, and we extracted the *t*-value and *p*-value estimated by the model for the
866 effect of slow-wave density or alpha power. Clusters of neighbouring electrodes were defined
867 as electrodes with *p*-values below .05 (cluster alpha). Once the clusters were defined, a
868 comparison was again performed with permuted datasets, and we used a Monte-Carlo *p*-value
869 threshold of .05 (one-sided test) to identify the significant clusters ($p_{cluster}$).

870 Finally, to be able to interpret null results obtained for VAS scores or behavioural
871 indexes of performances (misses, false alarms and reaction times), we computed the Bayes
872 Factor for the null hypothesis (BF_{01}) using Bayesian ANOVAs (fixed effect of drug treatment)
873 implemented in JASP (JASP 0.16). A BF_{01} above 3 is interpreted as significant evidence for
874 the null hypothesis.

875 **Graphical representation**

876 In Figure 2, 6a, S1 and S2, we used 'raincloud plots' to show the distribution of our variable
877 of interests at the sample level. These plots show a combination of boxplots, smoothed density
878 and individual datapoints. For boxplots, the central thick horizontal line shows the median, the
879 lower and upper limit of the box show the 1st and 3rd quartiles respectively, and the lower and
880 upper limit of the vertical lines (whiskers) show the minimum and maximum values
881 respectively. On the left-hand side of the boxplots, individual averages are shown as circles. A

882 smoothed density distribution is also shown on the right-hand side of the boxplots. These plots

883 were created with the raincloud plot package for R (Allen et al., 2021).

Acknowledgements

We thank Jessica Barnes for data collection. T.A. was supported by a 'Long-Term Fellowship' from the Human Frontier Science Program (LT000362/2018-L) and an 'Ideas Grant' from the National Health and Medical Research Council (APP2002454). R.G.O. was supported by a Horizon 2020 European Research Council Consolidator Grant IndDecision (865474). PD was supported by an Irish Research Council Laureate Grant (201911).

Competing Interests

The authors have no competing interests to declare.

Data and Code Availability Statement

All data will be made available by contacting the corresponding author. All code used for data analyses will be published online.

References

Allen M, Poggiali D, Whitaker K, Marshall TR, van Langen J, Kievit RA. 2021. Raincloud plots: a multi-platform tool for robust data visualization. *Wellcome Open Res* **4**:63. doi:10.12688/wellcomeopenres.15191.2

Andrillon T, Burns A, Mackay T, Windt J, Tsuchiya N. 2021. Predicting lapses of attention with sleep-like slow waves. *Nat Commun* **12**:3657. doi:10.1038/s41467-021-23890-7

Andrillon T, Kouider S. 2020. The vigilant sleeper: neural mechanisms of sensory (de)coupling during sleep. *Curr Opin Physiol* **15**:47–59. doi:10.1016/j.cophys.2019.12.002

Andrillon T, Windt J, Silk T, Drummond SPA, Bellgrove MA, Tsuchiya N. 2019. Does the mind wander when the brain takes a break? Local sleep in wakefulness, attentional lapses and mind-wandering. *Front Neurosci* **13**:949. doi:10.3389/fnins.2019.00949

Arnau S, Löffler C, Rummel J, Hagemann D, Wascher E, Schubert A. 2020. Inter-trial alpha power indicates mind wandering. *Psychophysiology* **57**. doi:10.1111/psyp.13581

Arnsten AF. 2010. The use of α-2A adrenergic agonists for the treatment of attention-deficit/hyperactivity disorder. *Expert Rev Neurother* **10**:1595–1605. doi:10.1586/ern.10.133

Arnsten AFT. 2000. Through the Looking Glass: Differential Noradenergic Modulation of Prefrontal Cortical Function. *Neural Plast* **7**:133–146. doi:10.1155/NP.2000.133

Arnsten AFT, Li B-M. 2005. Neurobiology of Executive Functions: Catecholamine Influences on Prefrontal Cortical Functions. *Biol Psychiatry* **57**:1377–1384. doi:10.1016/j.biopsych.2004.08.019

Arnsten AFT, Rubia K. 2012. Neurobiological Circuits Regulating Attention, Cognitive Control, Motivation, and Emotion: Disruptions in Neurodevelopmental Psychiatric Disorders. *J Am Acad Child Adolesc Psychiatry* **51**:356–367. doi:10.1016/j.jaac.2012.01.008

Aron AR, Dowson JH, Sahakian BJ, Robbins TW. 2003. Methylphenidate improves response inhibition in adults with attention-deficit/hyperactivity disorder. *Biol Psychiatry* **54**:1465–1468. doi:10.1016/S0006-3223(03)00609-7

Barnes JJM, O'Connell RG, Nandam LS, Dean AJ, Bellgrove MA. 2014. Monoaminergic modulation of behavioural and electrophysiological indices of error processing. *Psychopharmacology (Berl)* **231**:379–392. doi:10.1007/s00213-013-3246-y

Bates D, Mächler M, Bolker B, Walker S. 2015. Fitting Linear Mixed-Effects Models Using **lme4**. *J Stat Softw* **67**. doi:10.18637/jss.v067.i01

Bedard AC, Stein MA, Halperin JM, Krone B, Rajwan E, Newcorn JH. 2015. Differential impact of methylphenidate and atomoxetine on sustained attention in youth with attention-deficit/hyperactivity disorder. *J Child Psychol Psychiatry* **56**:40–48. doi:10.1111/jcpp.12272

Bernardi G, Siclari F, Yu X, Zennig C, Bellesi M, Ricciardi E, Cirelli C, Ghilardi MF, Pietrini P, Tononi G. 2015. Neural and behavioral correlates of extended training during sleep deprivation in humans: evidence for local, task-specific effects. *J Neurosci Off J Soc Neurosci* **35**:4487–4500. doi:10.1523/JNEUROSCI.4567-14.2015

Berridge CW, Devilbiss DM, Andrzejewski ME, Arnsten AFT, Kelley AE, Schmeichel B, Hamilton C, Spencer RC. 2006. Methylphenidate Preferentially Increases Catecholamine Neurotransmission within the Prefrontal Cortex at Low Doses that Enhance Cognitive Function. *Biol Psychiatry* **60**:1111–1120. doi:10.1016/j.biopsych.2006.04.022

Bond A, Lader M. 1974. The use of analogue scales in rating subjective feelings. *Br J Med Psychol* **47**:211–218. doi:10.1111/j.2044-8341.1974.tb02285.x

Borbély AA, Daan S, Wirz-Justice A, Deboer T. 2016. The two-process model of sleep regulation: a reappraisal. *J Sleep Res* **25**:131–143. doi:10.1111/jsr.12371

Boutrel B, Koob GF. 2004. What Keeps Us Awake: the Neuropharmacology of Stimulants and Wakefulness Promoting Medications. *Sleep* **27**:1181–1194. doi:10.1093/sleep/27.6.1181

Braboszcz C, Delorme A. 2011. Lost in thoughts: Neural markers of low alertness during mind wandering. *NeuroImage* **54**:3040–3047. doi:10.1016/j.neuroimage.2010.10.008

Bymaster F. 2002. Atomoxetine Increases Extracellular Levels of Norepinephrine and Dopamine in Prefrontal Cortex of Rat A Potential Mechanism for Efficacy in Attention Deficit/Hyperactivity Disorder. *Neuropsychopharmacology* **27**:699–711. doi:10.1016/S0893-133X(02)00346-9

Cajochen C, Brunner DP, Krauchi K, Graw P, Wirz-Justice A. 1995. Power density in theta/alpha frequencies of the waking EEG progressively increases during sustained wakefulness. *Sleep* **18**:890–894. doi:10.1093/sleep/18.10.890

Chamberlain SR, Hampshire A, Müller U, Rubia K, del Campo N, Craig K, Regenthal R, Suckling J, Roiser JP, Grant JE, Bullmore ET, Robbins TW, Sahakian BJ. 2009. Atomoxetine Modulates Right Inferior Frontal Activation During Inhibitory Control: A Pharmacological Functional Magnetic Resonance Imaging Study. *Biol Psychiatry* **65**:550–555. doi:10.1016/j.biopsych.2008.10.014

Clayton MS, Yeung N, Cohen Kadosh R. 2018. The many characters of visual alpha oscillations. *Eur J Neurosci* **48**:2498–2508. doi:10.1111/ejn.13747

Compton RJ, Gearinger D, Wild H. 2019. The wandering mind oscillates: EEG alpha power is enhanced during moments of mind-wandering. *Cogn Affect Behav Neurosci* **19**:1184–1191. doi:10.3758/s13415-019-00745-9

Connell RG, Dockree PM, Robertson IH, Bellgrove MA, Foxe JJ, Kelly SP. 2009. Uncovering the neural signature of lapsing attention: Electrophysiological signals predict errors up to 20 s before they occur. *J Neurosci* **29**:8604–8611. doi:10.1523/JNEUROSCI.5967-08.2009

Conners CK, Erhardt D, Epstein JN, Parker JDA, Sitarenios G, Sparrow E. 1999. Self-ratings of ADHD symptoms in adults I: Factor structure and normative data. *J Atten Disord* **3**:141–151. doi:10.1177/108705479900300303

Cortese S. 2020. Pharmacologic Treatment of Attention Deficit–Hyperactivity Disorder. *N Engl J Med* **383**:1050–1056. doi:10.1056/NEJMra1917069

D'Ambrosio S, Castelnovo A, Guglielmi O, Nobili L, Sarasso S, Garbarino S. 2019. Sleepiness as a Local Phenomenon. *Front Neurosci* **13**:1086. doi:10.3389/fnins.2019.01086

Dimitrijevic A, Smith ML, Kadis DS, Moore DR. 2017. Cortical alpha oscillations predict speech intelligibility. *Front Hum Neurosci* **11**. doi:10.3389/fnhum.2017.00088

Ding YS, Naganawa M, Gallezot JD, Nabulsi N, Lin SF, Ropchan J, Weinzimmer D, McCarthy TJ, Carson RE, Huang Y, Laruelle M. 2014. Clinical doses of atomoxetine significantly occupy both norepinephrine and serotonin transports: Implications on treatment of depression and ADHD. *NeuroImage* **86**:164–71. doi:10.1016/j.neuroimage.2013.08.001

Dockree PM, Barnes JJ, Matthews N, Dean AJ, Abe R, Nandam LS, Kelly SP, Bellgrove MA, O'Connell RG. 2017. The Effects of Methylphenidate on the Neural Signatures of Sustained Attention. *Biol Psychiatry* **82**:687–694. doi:10.1016/j.biopsych.2017.04.016

Doran SM, Van Dongen HP, Dinges DF. 2001. Sustained attention performance during sleep deprivation: evidence of state instability. *Arch Ital Biol* **139**:253–267.

Esterman M, Rothlein D. 2019. Models of sustained attention. *Curr Opin Psychol* **29**:174–180. doi:10.1016/j.copsyc.2019.03.005

Farr OM, Zhang S, Hu S, Matuskey D, Abdelghany O, Malison RT, Li CR. 2014. The effects of methylphenidate on resting-state striatal, thalamic and global functional connectivity in healthy adults. *Int J Neuropsychopharmacol* **17**:1177–1191. doi:10.1017/S1461145714000674

Geissler J, Romanos M, Hegerl U, Hensch T. 2014. Hyperactivity and sensation seeking as autoregulatory attempts to stabilize brain arousal in ADHD and mania? *ADHD Atten Deficit Hyperact Disord* **6**:159–173. doi:10.1007/s12402-014-0144-z

Gelbard-Sagiv H, Magidov E, Sharon H, Hendler T, Nir Y. 2018. Noradrenaline Modulates Visual Perception and Late Visually Evoked Activity. *Curr Biol* **28**:2239-2249.e6. doi:10.1016/j.cub.2018.05.051

Graf H, Abler B, Freudenmann R, Beschoner P, Schaeffeler E, Spitzer M, Schwab M, Grön G. 2011. Neural Correlates of Error Monitoring Modulated by Atomoxetine in Healthy Volunteers. *Biol Psychiatry* **69**:890–897. doi:10.1016/j.biopsych.2010.10.018

Hung CS, Sarasso S, Ferrarelli F, Riedner B, Ghilardi MF, Cirelli C, Tononi G. 2013. Local experience-dependent changes in the wake EEG after prolonged wakefulness. *Sleep* **36**:59–72. doi:10.5665/sleep.2302

Janssen TWP, Bink M, Geladé K, van Mourik R, Maras A, Oosterlaan J. 2016. A randomized controlled trial into the effects of neurofeedback, methylphenidate, and physical activity on EEG power spectra in children with ADHD. *J Child Psychol Psychiatry* **57**:633–644. doi:10.1111/jcpp.12517

Jensen O, Mazaheri A. 2010. Shaping Functional Architecture by Oscillatory Alpha Activity: Gating by Inhibition. *Front Hum Neurosci* **4**. doi:10.3389/fnhum.2010.00186

Jones BE. 2005. From waking to sleeping: Neuronal and chemical substrates. *Trends Pharmacol Sci* **26**:578–586. doi:10.1016/j.tips.2005.09.009

Jouvet M. 1999. Sleep and Serotonin An Unfinished Story. *Neuropsychopharmacology* **21**:24S-27S. doi:10.1016/S0893-133X(99)00009-3

Kalauzi A, Vuckovic A, Bojić T. 2012. EEG alpha phase shifts during transition from wakefulness to drowsiness. *Int J Psychophysiol* **86**:195–205. doi:10.1016/j.ijpsycho.2012.04.012

Kappenman ES, Luck SJ. 2011. ERP components: The ups and downs of brainwave recordings. OUP.

Killingsworth MA, Gilbert DT. 2010. A Wandering Mind Is an Unhappy Mind. *Science* **330**:932–932. doi:10.1126/science.1192439

Klimesch W. 2012. Alpha-band oscillations, attention, and controlled access to stored information. *Trends Cogn Sci* **16**:606–617. doi:10.1016/j.tics.2012.10.007

Klimesch W, Fellinger R, Freunberger R. 2011. Alpha Oscillations and Early Stages of Visual Encoding. *Front Psychol* **2**. doi:10.3389/fpsyg.2011.00118

Koda K, Ago Y, Cong Y, Kita Y, Takuma K, Matsuda T. 2010. Effects of acute and chronic administration of atomoxetine and methylphenidate on extracellular levels of noradrenaline, dopamine and serotonin in the prefrontal cortex and striatum of mice: Acute and chronic treatment with ADHD drugs. *J Neurochem* no-no. doi:10.1111/j.1471-4159.2010.06750.x

Kowalczyk OS, Cubillo AI, Smith A, Barrett N, Giampietro V, Brammer M, Simmons A, Rubia K. 2019. Methylphenidate and atomoxetine normalise fronto-parietal underactivation during sustained attention in ADHD adolescents. *Eur Neuropsychopharmacol* **29**:1102–1116. doi:10.1016/j.euroneuro.2019.07.139

Lee S-H, Dan Y. 2012. Neuromodulation of Brain States. *Neuron* **76**:209–222. doi:10.1016/j.neuron.2012.09.012

Liljeholm M, O'Doherty JP. 2012. Contributions of the striatum to learning, motivation, and performance: an associative account. *Trends Cogn Sci* **16**:467–475. doi:10.1016/j.tics.2012.07.007

Lufi D, Bassin-Savion S, Rubel L. 2015. The effect of methylphenidate on sustained attention among adolescents with attention-deficit hyperactivity disorder. *Neurocase* **21**:802–808. doi:10.1080/13554794.2015.1023317

Macdonald JSP, Mathan S, Yeung N. 2011. Trial-by-Trial Variations in Subjective Attentional State are Reflected in Ongoing Prestimulus EEG Alpha Oscillations. *Front Psychol* **2**. doi:10.3389/fpsyg.2011.00082

Macmillan NA. 1993. Signal detection theory as data analysis method and psychological decision model In: Keren G, Lewis C, editors. A Handbook for Data Analysis in the Behavioral Sciences: Methodological Issues. Lawrence Erlbaum Associates, Inc. pp. 21–57.

Maffei A, Angrilli A. 2018. Spontaneous eye blink rate: An index of dopaminergic component of sustained attention and fatigue. *Int J Psychophysiol* **123**:58–63. doi:10.1016/j.ijpsycho.2017.11.009

Maris E, Oostenveld R. 2007. Nonparametric statistical testing of EEG- and MEG-data. *J Neurosci Methods* **164**:177–190. doi:10.1016/j.jneumeth.2007.03.024

McKie S, Del-Ben C, Elliott R, Williams S, del Vai N, Anderson I, Deakin JFW. 2005. Neuronal effects of acute citalopram detected by pharmacoMRI. *Psychopharmacology (Berl)* **180**:680–686. doi:10.1007/s00213-005-2270-y

Mignot EJM. 2012. A Practical Guide to the Therapy of Narcolepsy and Hypersomnia Syndromes. *Neurotherapeutics* **9**:739–752. doi:10.1007/s13311-012-0150-9

Milne RJ, Goa KL. 1991. Citalopram: A Review of its Pharmacodynamic and Pharmacokinetic Properties, and Therapeutic Potential in Depressive Illness. *Drugs* **41**:450–477. doi:10.2165/00003495-199141030-00008

Mittner M, Hawkins GE, Boekel W, Forstmann BU. 2016. A neural model of mind wandering. *Trends Cogn Sci* **20**:570–578. doi:10.1016/j.tics.2016.06.004

Nandam LS, Hester R, Bellgrove MA. 2014. Dissociable and common effects of methylphenidate, atomoxetine and citalopram on response inhibition neural networks. *Neuropsychologia* **56**:263–270. doi:10.1016/j.neuropsychologia.2014.01.023

Nandam LS, Hester R, Wagner J, Cummins TDR, Garner K, Dean AJ, Kim BN, Nathan PJ, Mattingley JB, Bellgrove MA. 2011. Methylphenidate But Not Atomoxetine or Citalopram Modulates Inhibitory Control and Response Time Variability. *Biol Psychiatry* **69**:902–904. doi:10.1016/j.biopsych.2010.11.014

Nir Y, Andrillon T, Marmelshtein A, Suthana N, Cirelli C, Tononi G, Fried I. 2017. Selective neuronal lapses precede human cognitive lapses following sleep deprivation. *Nat Med* **23**:1474–1480. doi:10.1038/nm.4433

Nobili L, De Gennaro L, Proserpio P, Moroni F, Sarasso S, Pigorini A, De Carli F, Ferrara M. 2012. Local aspects of sleep: Observations from intracerebral recordings in humans. *Prog Brain Res* **199**:219–232. doi:10.1016/B978-0-444-59427-3.00013-7

Norris H. 1971. The action of sedatives on brain stem oculomotor systems in man. *Neuropharmacology* **10**:181–191. doi:10.1016/0028-3908(71)90039-6

O'Connell RG, Dockree PM, Robertson IH, Bellgrove MA, Foxe JJ, Kelly SP. 2009. Uncovering the Neural Signature of Lapsing Attention: Electrophysiological Signals Predict Errors up to 20 s before They Occur. *J Neurosci* **29**:8604–8611. doi:10.1523/JNEUROSCI.5967-08.2009

Oikonomou G, Altermatt M, Zhang RW, Coughlin GM, Montz C, Gradinaru V, Prober DA. 2019. The serotonergic raphe promote sleep in zebrafish and mice. *Neuron* **103**:686-701.e8. doi:10.1016/j.neuron.2019.05.038

Oken BS, Salinsky MC, Elsas SM. 2006. Vigilance, alertness, or sustained attention: Physiological basis and measurement. *Clin Neurophysiol* **117**:1885–1901. doi:10.1016/j.clinph.2006.01.017

Oostenveld R, Fries P, Maris E, Schoffelen J-M. 2011. FieldTrip: Open Source Software for Advanced Analysis of MEG, EEG, and Invasive Electrophysiological Data. *Comput Intell Neurosci* **2011**:1–9. doi:10.1155/2011/156869

Owens JA. 2005. The ADHD and Sleep Conundrum: A Review. *J Dev Behav Pediatr* **26**:312–322. doi:10.1097/00004703-200508000-00011

Parasuraman R. 1979. Memory Load and Event Rate Control Sensitivity Decrements in Sustained Attention. *Science* **205**:924–927. doi:10.1126/science.472714

Peylo C, Hilla Y, Sauseng P. 2021. Cause or consequence? Alpha oscillations in visuospatial attention. *Trends Neurosci* **44**:705–713. doi:10.1016/j.tins.2021.05.004

Pfurtscheller G. 1992. Event-related synchronization (ERS): an electrophysiological correlate of cortical areas at rest. *Electroencephalogr Clin Neurophysiol* **83**:62–69. doi:10.1016/0013-4694(92)90133-3

Pfurtscheller G, Stancák A, Neuper C. 1996. Event-related synchronization (ERS) in the alpha band - An electrophysiological correlate of cortical idling: A review. *Int J Psychophysiol* **24**:39–46.

Polich J. 2007. Updating P300: An integrative theory of P3a and P3b. *Clin Neurophysiol* **118**:2128–2148. doi:10.1016/j.clinph.2007.04.019

Quercia A, Zappasodi F, Committeri G, Ferrara M. 2018. Local use-dependent sleep in wakefulness links performance errors to learning. *Front Hum Neurosci* **12**:122. doi:10.3389/fnhum.2018.00122

Ranjbar-Slamloo Y, Fazlali Z. 2020. Dopamine and Noradrenaline in the Brain; Overlapping or Dissociate Functions? *Front Mol Neurosci* **12**:334. doi:10.3389/fnmol.2019.00334

Riedner BA, Vyazovskiy VV, Huber R, Massimini M, Esser S, Murphy M, Tononi G. 2007. Sleep homeostasis and cortical synchronization: III. A high-density EEG study of sleep slow waves in humans. *Sleep* **30**:1643–57.

Riley E, Esterman M, Fortenbaugh FC, DeGutis J. 2017. Time-of-day variation in sustained attentional control. *Chronobiol Int* **34**:993–1001. doi:10.1080/07420528.2017.1308951

Robbins TW. 1997. Arousal systems and attentional processes. *Biol Psychol* **45**:57–71. doi:10.1016/S0301-0511(96)05222-2

Romei V, Brodbeck V, Michel C, Amedi A, Pascual-Leone A, Thut G. 2008. Spontaneous Fluctuations in Posterior -Band EEG Activity Reflect Variability in Excitability of Human Visual Areas. *Cereb Cortex* **18**:2010–2018. doi:10.1093/cercor/bhm229

Ross JA, Van Bockstaele EJ. 2021. The Locus Coeruleus- Norepinephrine System in Stress and Arousal: Unraveling Historical, Current, and Future Perspectives. *Front Psychiatry* **11**:601519. doi:10.3389/fpsyt.2020.601519

Samaha J, Gosseries O, Postle BR. 2017. Distinct Oscillatory Frequencies Underlie Excitability of Human Occipital and Parietal Cortex. *J Neurosci* **37**:2824–2833. doi:10.1523/JNEUROSCI.3413-16.2017

Sara SJ. 2009. The locus coeruleus and noradrenergic modulation of cognition. *Nat Rev Neurosci* **10**:211–223. doi:10.1038/nrn2573

Sara SJ, Bouret S. 2012. Orienting and reorienting: The locus coeruleus mediates cognition through arousal. *Neuron* **76**:130–141. doi:10.1016/j.neuron.2012.09.011

Satterfield JH, Dawson ME. 1971. ELECTRODERMAL CORRELATES OF HYPERACTIVITY IN CHILDREN. *Psychophysiology* **8**:191–197. doi:10.1111/j.1469-8986.1971.tb00450.x

Sauer JM, Ring BJ, Witcher JW. 2005. Clinical pharmacokinetics of atomoxetine. *Clin Pharmacokinet* **44**:571–590. doi:10.2165/00003088-200544060-00002

Schmitt JAJ, Ramaekers JG, Kruizinga MJ, van Boxtel MPJ, Vuurman EFPM, Riedel WJ. 2002. Additional dopamine reuptake inhibition attenuates vigilance impairment induced by serotonin reuptake inhibition in man. *J Psychopharmacol (Oxf)* **16**:207–214. doi:10.1177/026988110201600303

Sheehan DV, Lecrubier Y, Sheehan KH, Amorim P, Janavs J, Weiller E, Hergueta T, Baker R, Dunbar GC. 1998. The Mini-International Neuropsychiatric Interview (M.I.N.I.): The development and validation of a structured diagnostic psychiatric interview for DSM-IV and ICD-10. *J Clin Psychiatry* **59 Suppl 20**:22-33;quiz 34-57.

Smallwood J, Brown KS, Tipper C, Giesbrecht B, Franklin MS, Mrazek MD, Carlson JM, Schooler JW. 2011. Pupillometric Evidence for the Decoupling of Attention from Perceptual Input during Offline Thought. *PLoS ONE* **6**:e18298. doi:10.1371/journal.pone.0018298

Smallwood J, Schooler JW. 2015. The Science of Mind Wandering: Empirically Navigating the Stream of Consciousness. *Annu Rev Psychol* **66**:487–518. doi:10.1146/annurev-psych-010814-015331

Solanto MV. 1998. Neuropsychopharmacological mechanisms of stimulant drug action in attention-deficit hyperactivity disorder: a review and integration. *Behav Brain Res* **94**:127–152. doi:10.1016/S0166-4328(97)00175-7

Sparks DW, Tian MK, Sargin D, Venkatesan S, Intson K, Lambe EK. 2018. Opposing Cholinergic and Serotonergic Modulation of Layer 6 in Prefrontal Cortex. *Front Neural Circuits* **11**:107. doi:10.3389/fncir.2017.00107

Spencer SV, Hawk LW, Richards JB, Shiels K, Pelham WE, Waxmonsky JG. 2009. Stimulant Treatment Reduces Lapses in Attention among Children with ADHD: The Effects of Methylphenidate on Intra-Individual Response Time Distributions. *J Abnorm Child Psychol* **37**:805–816. doi:10.1007/s10802-009-9316-2

Sturm W, Willmes K. 2001. On the Functional Neuroanatomy of Intrinsic and Phasic Alertness. *NeuroImage* **14**:S76–S84. doi:10.1006/nimg.2001.0839

Thiele A, Bellgrove MA. 2018. Neuromodulation of Attention. *Neuron* **97**:769–785. doi:10.1016/j.neuron.2018.01.008

van Schie MKM, Lammers GJ, Fronczek R, Middelkoop HAM, van Dijk JG. 2021. Vigilance: discussion of related concepts and proposal for a definition. *Sleep Med* **83**:175–181. doi:10.1016/j.sleep.2021.04.038

Volkow ND, Wang G-J, Tomasi D, Kollins SH, Wigal TL, Newcorn JH, Telang FW, Fowler JS, Logan J, Wong CT, Swanson JM. 2012. Methylphenidate-Elicited Dopamine Increases in Ventral Striatum Are Associated with Long-Term Symptom Improvement in Adults with Attention Deficit Hyperactivity Disorder. *J Neurosci* **32**:841–849. doi:10.1523/JNEUROSCI.4461-11.2012

Vyazovskiy VV, Olcese U, Hanlon EC, Nir Y, Cirelli C, Tononi G. 2011. Local sleep in awake rats. *Nature* **472**:443–447. doi:10.1038/nature10009

Ward AF, Wegner DM. 2013. Mind-blanking: When the mind goes away. *Front Psychol* **4**:650. doi:10.3389/fpsyg.2013.00650

Wingen M, Kuypers KPC, van de Ven V, Formisano E, Ramaekers JG. 2008. Sustained attention and serotonin: A pharmaco-fMRI study. *Hum Psychopharmacol Clin Exp* **23**:221–230. doi:10.1002/hup.923

Supplementary Figures

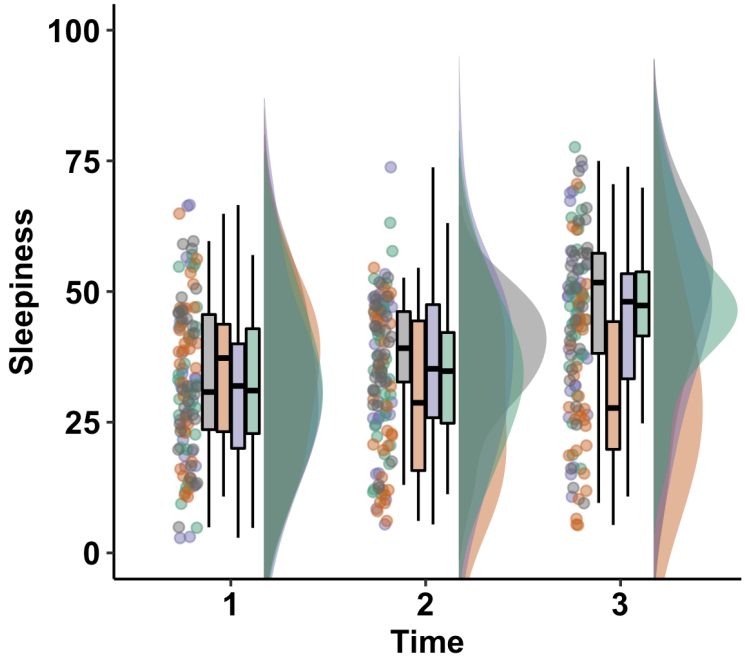

Supplementary Figure 1. Effect of treatments of subjective sleepiness

Participants were asked to complete a visual analogue scale (VAS) about their subjective sleepiness at three time points during each recording session: at drug administration (t=0 minutes), before the CTET (t=90 minutes) and after the CTET (t=180 minutes). The raincloud plot (see Methods) for each drug treatment (PLA: grey, MPH: orange, ATM: purple, CIT: green) and time is shown.

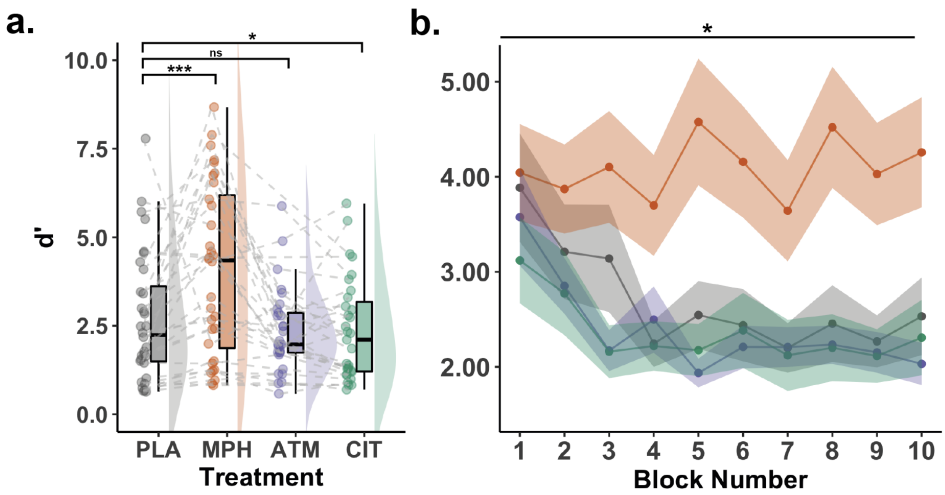

Supplementary Figure 2. Effect of treatments on behavioural performance (d')

We computed an index of behavioural performance integrating correctness on both target and non-target trials: the d' (see Methods). ***a****: Sample and individual averages (PLA: N=32; CIT: N=31; ATM: N=31; and MPH: N=32 individuals) computed across all CTET blocks (N=10 blocks) for each treatment. The raincloud plot (see Methods) for each drug treatment (PLA: grey, MPH: orange, ATM: purple, CIT: green) is shown. Stars denote the significance level (ns: non-significant; (*): p < .05; (**): p < .01; (***): p < .001) of the difference between placebo and the three treatments used in this protocol (MPH vs PLA, ATM vs PLA, CIT vs PLA), as determined by a linear mixed-effect model (see Methods).* ***b****: Sample averages (circles) and standard-error of the mean (coloured areas) across participants for each drug treatment and block (N=10 blocks). The star denotes the significance level (*: p < .05) of the interaction between block number and drug treatment, as determined by a linear mixed-effect model.*

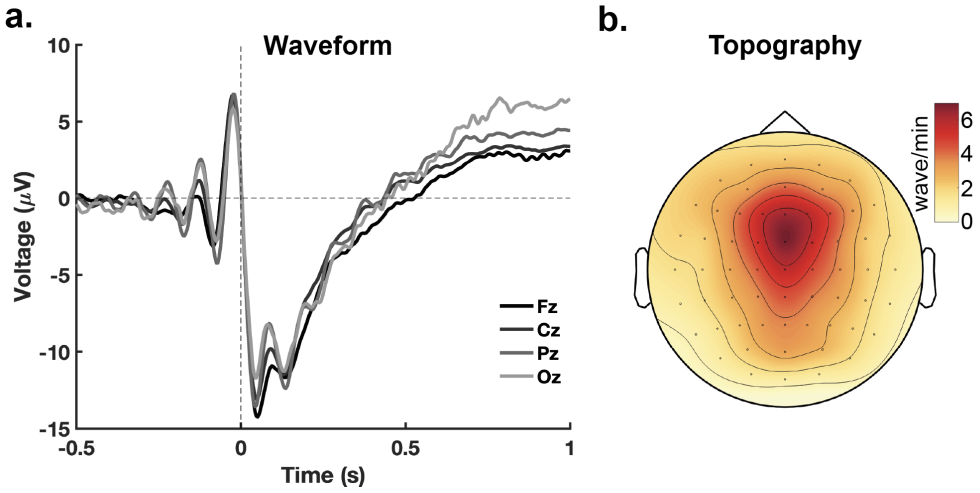

Supplementary Figure 3. Slow waves' waveform and spatial distribution

a: *We computed the average waveforms of the detected slow waves for a selection of midline electrodes (Frontal (Fz), Central (Cz), Parietal (Pz), and Occipital (Oz)) on a [-0.5, 1]s window. Slow waves were aligned according to their first negative zero-crossing and baseline using a [-0.5, 0]s window. The temporal profiles shown here are the averages across all participants (N=32).* ***b***: *Topographical map showing the spatial distribution of slow waves. We extracted slow-wave density (wave/min) per electrode and show here the average across participants.*